ADVANCED SENSORS AND INSTRUMENTATION

Issue 12 • March 2020

Update on NEET ASI Advanced Instrumentation Development Activities

Pattrick Calderoni,
Idaho National Laboratory

Instruments are the foundational and enabling component of instrumentation and control (I&C) systems. An instrument is the technological application of measurement science principles and methods, combining sensors (or sensing elements) with all the necessary auxiliary components necessary to provide a measured parameter to the I&C system. Existing nuclear plants utilize a wide range of instruments that provide data at varying temporal and spatial resolutions to support operations and maintenance. In addition, instruments are a key enabling component of demonstration tests for advanced nuclear components (nuclear fuel and materials, primary loop circulation pumps, heat exchangers, etc.) and advanced reactor concepts (e.g., microreactor core flow distribution).

The objective of the advanced instrumentation research area is to provide reliable, real-time, cost-effective, accurate, high-resolution performance measurement of existing and advanced reactor core and plant systems. Instruments are designed, fabricated, and tested in relevant and operational conditions to advance their technological readiness to the point that they can be integrated into I&C systems without the significant costs and risks associated with development activities.

The development of reactor core (in-pile) instruments for material test reactor (MTR) experiments is an important component of the program's objective due to the limitations of available commercial solutions and the impact they could have on the acceleration of nuclear system component demonstrations. In addition, the capability of testing developmental instruments in MTRs is critical for demonstrating their performance in relevant and operational conditions.

The extensive deployment of advanced instrumentation in irradiation experiments is the most effective path to their technological maturation and consequent adoption by program stakeholders. This is true not only for adoption by other Department of Energy Office of Nuclear Energy (DOE-NE) programs, but also for advanced reactor designers and end users for whom demonstrations in relevant conditions and the accumulation of performance and reliability data is a crucial step for allowing integration into the I&C system and contributing to the plant licensing case. It should be noted that the conditions of a given MTR irradiation experiment vary widely, depending on the

Continued on next page

In this issue...

Continued from previous page

test facility and the scope of the experiment's duration, core position, etc.; thus, they can be relevant to demonstrations of instruments targeting either the core or other plant systems.

The implementation of research activities is organized into three main categories:

1. The development of instruments to measure plant operational parameters (in- and ex-core), such as neutron flux, temperature, and pressure. Instruments are designed and demonstrated in MTR irradiation experiments, but ultimately adopted by program stakeholders for integration into the I&C systems of advanced nuclear plants. The primary path to close the technologies' lifecycles within the NEET ASI program is through commercialization.
2. The development of measurement systems for real-time characterization of nuclear fuel and material properties in MTR tests. These activities are derived from analyses of existing gaps performed in collaboration with DOE nuclear fuel and materials development programs and include the measurement of material's properties (thermal and mechanical properties, chemistry), the characterization of its microstructure, and the prediction of its behavior through modeling and simulations. The primary path to close the technologies' lifecycles within the NEET ASI program is via adoption by the other DOE-NE programs. However, commercialization of novel instruments for component lifetime prediction (instruments for non-destructive examination, early fault detection, etc.) is also expected.
3. The development of testing systems to demonstrate instrumentation performance in relevant and operational conditions. The primary focus is on irradiation experiments in MTRs, as previously discussed. However, out-of-pile tests are also included when necessary to satisfy the requirements for deployment in MTRs. The capability of installing instruments on irradiated fuel rods and the development of a test rig for performance demonstration of instruments in the Advanced Test Reactor and High-Flux Isotope Reactor are considered key elements in implementing the program's mission.

Direct-funded research and development activities implemented in FY 2020 as part of NEET ASI for the three categories above are listed in Table 1. Technical details for some of the activities are included in this newsletter.

Table 1. FY 2020 NEET ASI direct-funded projects. Highlighted in blue are projects with summaries included in this newsletter.

Nuclear instrumentation to measure plant operational parameters	• Thermocouples • Neutron flux sensors • Passive monitors • Acoustic sensors • Optical fibers • Wireless communication • Advanced manufacturing
Measurement systems for real-time characterization of nuclear fuel and material properties	• Mechanical properties • Photo-thermal radiometry • Probe method • Resonant Ultrasound Spectroscopy • Electrochemical measurements
Testing systems to demonstrate instrumentation performance in relevant and operational conditions	• Autoclave test • Fuel re-instrumentation facility • Irradiation test

High-Temperature Irradiation-Resistant Thermocouples

Richard Skifton, PhD
Idaho National Laboratory

Introduction

The High-Temperature Irradiation-Resistant Thermocouple (HTIR-TC) is generally the world's leading temperature sensor for reactor fuel experiments and material test reactors (Advanced Test Reactor, Massachusetts Institute of Technology Nuclear Reactor, etc.). Recently commercialized, the HTIR-TC provides real-time centerline and fuel cladding temperature measurements of reactor fuel experiments during irradiations. This provides direct information about fuel temperatures during Generation-IV reactors, small modular reactors, and microreactor vetting processes. Further, the HTIR-TC recently won the 2019 R&D100 award under category: Analytical/Test.

The Temperature Gap

Between 1100°C and 1700°C, it can be difficult to find the right thermocouple, particularly for use in radiation environments. Lower temperature thermocouples are at the upper end of their optimal performance in this range, yet higher temperature thermocouples like tungsten/rhenium are at their lower operating temperature range. Platinum/rhodium thermocouples that are best suited for this temperature range experience drift and failures associated with metallurgical phenomena, such as transmutation, solid state diffusion, selective evaporation, and recrystallization. The HTIR-TC works with the refractory metals molybdenum (+) and niobium (-) to overcome these setbacks. Both have high melting points, are easy to work with, and have relatively very low neutron absorption cross sections.

Reactor In-pile HTIR-TC Results

The HTIR-TC was recently inserted into the Advanced Test Reactor during the Advanced Gas Reactor 5/6/7 test and showed resiliency to the irradiation and high temperatures experienced. See Figure 1 for temperature results of HTIR-TCs compared to Type N TCs that were within close proximity to each other in the tests. One particular HTIR-TC (i.e., TC5 in Figure 1) located at the geometric center of the nuclear fuel (i.e., the highest temperature location) held temperatures up 1510°C consistently for approximately 9 weeks of full reactor power—that is equivalent to 12 full months. Further, the intermittent reactor shutdowns and restarts inherent in this type of experiment put the HTIR-TC through severe temperature transients. Each time that the reactor restarted, the reading would resume as normal. Other HTIR-TCs in the vicinity have held temperatures of 1200°C–1350°C. It was noted that at higher temperatures the HTIR-TCs outperformed the Type N TCs .

Continued on next page

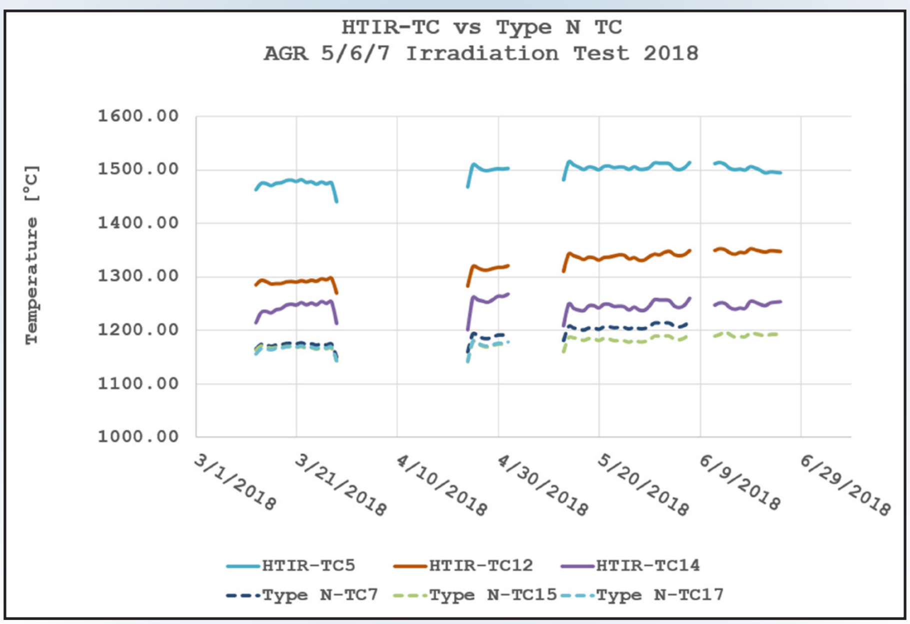

Figure 1. A small window of data for the AGR 5/6/7 results of HTIR-TCs and Type N TCs; showing the HTIR-TCs outlasted and outperformed the Type N TCs in near vicinity.

Continued from previous page

Table 1 shows the comparative temperature ranges, cost, and materials of other commercially available thermocouples currently used in high-temperature operations, reactor experiments, or both. The HTIR-TC bring together the idea of high-temperature and irradiation resistance that no other thermocouple can. In fact, the HTIR-TC thermoelements are about 4× more "rad-hardened" than the Type N TC.

Traditional vs. Optimized Design

The HTIR-TC has been constructed using both the traditional methods (i.e., mineral insulated metal sheathed two-wire configuration) and a new robust single wire methodology (e.g., coaxial) using the sheath material as the second thermoelement (see Figure 2). The latter makes for a smaller diameter unit with longer length than the traditional means, the material is also more robust and less prone to artificial junctions upon overheating.

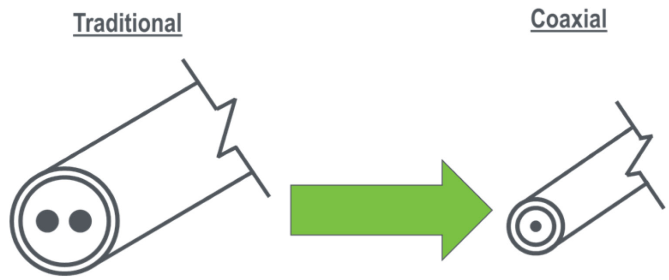

Figure 2. Traditional HTIR-TC mineral insulated metal sheathed cabling versus the optimized "coaxial" cabling. The coaxial cable provides builds with longer lengths, smaller diameters, and more robust performance.

Conclusion

As the name suggests, the HTIR-TC is a world record holder in temperature measurements, specifically inside high-temperature, irradiation environments. Sustaining long-duration temperature readings—consistently and reliably—inside a high-neutron flux environment at temperatures exceeding 1500°C for months on end. Further, the robust optimized design of coaxial cabling means the HTIR-TC can last for longer periods of time without any significant drift (decalibration).

Table 1. Comparative table of standard thermocouples versus HITR-TC used within reactor environment.

Thermocouple:	Type K	Type B	Type N	HTIR-TC
Materials	Nickel Chromium vs. Nickel Alumel	Platinum-Rhodium 30% vs. Platinum-Rhodium 6%	Nicrosil vs. Nisil	Molybdenum vs. Niobium (Coaxial)
Temperature Range	-270°C to 1260°C	0°C to 1700°C	-270°C to 1260°C	0°C to 1700°C
Cost	~$30/ft	~$250/ft	~$50/ft	~$250/ft ($100/ft)
Irradiation Tolerant?	No	No	No	Yes

Evaluations of Silicon Carbide Temperature Monitors

Malwina Wilding
Idaho National Laboratory

Introduction

The effect of irradiation on materials properties is an important field of study for materials usage in both fission and fusion systems for energy production. Neutron flux and energy spectrums are well understood; however, the irradiation temperature can be more difficult to determine. Since the early 1960s, silicon carbide (SiC) has been used as a passive post-irradiation temperature monitor because the irradiation defects anneal out above the irradiation temperature. [1-3] Irradiation temperature is determined by measuring a property change after isochronal annealing or during a continuously monitored annealing process. [1-3] Many properties may be measured, including electrical resistivity, bulk density, dimensions, thermal diffusivity, or lattice spacing. Electrical resistivity is accepted as a robust measurement technique; however, such method is time-consuming since the steps involved must be performed in a serial manner. [4-5] The use of thermal expansion from continuous dilatometry is an automated process requiring minimal setup time. [4-5] As part of a Nuclear Science User Facilities project, low-dose silicon carbide monitors were irradiated in the Belgian Reactor 2 (BR2) material test reactor at *Studiecentrum voor Kernenergie (*SCK), Belgium. These samples were then evaluated at the Idaho National Laboratory High-Temperature Test Laboratory (HTTL) to determine their peak temperature achieved during irradiation. The technical significance of this work is that the total dose of the irradiated monitors is significantly less than that recommended in published literature. This paper will discuss the evaluation processes available at HTTL to read peak irradiation temperature of passive monitors. [1-2]

Methodology

In the first method, HTTL used resistivity measurements to find the peak irradiation temperature. The SiC monitors are heated in the annealing furnace using isochronal temperature steps. After each isochronal annealing, the specimens are placed in a resistance measurement fixture located in the constant temperature chamber (maintained at 40°C) for a minimum of 30 minutes. An ohmic response curve is generated for each monitor prior to heating. The peak irradiation temperature, using an electrical resistivity technique, can be taken as the point where the resistivity begins and consistently remains, above the error band. For this evaluation, the error band was established as the ±2σ value based on a sample size of the first five data points taken below 150°C. [1-2]

Figure 1. SiC temperature monitors available for use in irradiation testing include small rods and discs. Monitors photographed with U.S. cent for size perspective. [1]

In the second method, Idaho National Laboratory researchers developed a method aimed at using electrical resistance measured during a two-pass heating-cooling cycle as a means of recovering the irradiation temperature of a SiC monitor. A fully automated means of using continuous measurement of resistance of SiC monitors during heating/cooling has been developed and involves relatively inexpensive resistance measuring equipment. To minimize thermal perturbations, which increase uncertainty in the temperature measurement, a constant heating rate is applied during the measurements above 150°C. Results indicate that the relationship between resistance and temperature of a SiC monitor shows a significant change in resistance difference slope when the peak irradiation temperature is reached. [3]

Continued on next page

Continued from previous page

Finally, the last method uses thermal expansion from continuous dilatometry, which is an automated process requiring minimal setup and run time. This method uses an optical dilatometer that requires no contact with samples, eliminates the need for measurement calibrations and corrections, and requires only one measurement run to determine irradiation temperatures. Moreover, there has been only very limited reports on the effect of irradiation on the thermal expansion behavior of SiC. The historical inability to implement this process was most likely due to limited resolution of the dilatometers and lack of statistical analysis methods. This dilatometer has a very high resolution that produces continuous measurement of length/diameter. To achieve similar anticipated error range in determining irradiation temperature as previous methods discussed, ramp rates smaller than ~2.5 K/min for the dilatometry-based thermometry is recommended. Limited yet significant improvement in accuracy may be achieved by further decreasing the ramp rate. [4-5]

Conclusion

SiC temperature monitors were irradiated in BR2 as part of an Nuclear Science User Facilities project and were evaluated at the HTTL using multiple evaluation methods to determine their peak irradiation temperatures. The peak irradiation temperature of each monitor was evaluated using the resistance measurement method, an automated resistivity method, and dilatometry-based thermometry method. Deviations between the calculated temperature and the evaluated temperature were within or near published limits for all methods. A significant finding from this evaluation is that it is possible to evaluate SiC temperature monitors at dose levels much less than 1 dpa. SiC monitors were successfully evaluated that were irradiated to 0.5 dpa with temperatures ranging from 240°C to 380°C. [1-2]

References

[1] Davis, K. L., et al. "Evaluation of Low Dose Silicon Carbide Temperature Monitors," IEEE Transactions on Nuclear Science, 2019, pp. 1–1, doi:10.1109/tns.2019.2957972.

[2] Davis, K. L., and T. C. Unruh, "Silicon Carbide Temperature Monitor Evaluation." PLN-3473, Rev. 2, Idaho National Laboratory, February 2018.

[3] Al Rashdan, A., K. Davis, T. Unruh, and J. Daw, "Silicon Carbide Temperature Monitor Online Evaluation," PLN-5465, Idaho National Laboratory, September 2017.

[4] Field, K. G., J. L. McDuffee, J. W. Geringer, C. M. Petrie, Y. Katoh, "Evaluation of the Continuous Dilatometer Method of Silicon Carbide Thermometry for Passive Irradiation Temperature Determination," Nuclear Instruments and Methods in Physics Research Section B: Beam Interactions with Materials and Atoms, Vol. 445, April 15, 2019, pp. 46–56.

[5] Campbell, A. A., W. D. Porter, Y. Katoh, and L. L. Snead, "Method for Analyzing Passive Silicon Carbide Thermometry with a Continuous Dilatometer to Determine Irradiation Temperature," Nuclear Instruments and Methods in Physics Research Section B: Beam Interactions with Materials and Atoms, Vol. 370, March 2016, pp. 49–58.

Development of an Electrochemical Impedance Instrument for In-pile Monitoring Cladding Materials Behaviors

Austin Fleming
Idaho National Laboratory

Ashley Lambson
Idaho National Laboratory

Colby Jensen
Idaho National Laboratory

Introduction

Measurements from in-core instrumentation are some of the most demanding and challenging environments that exist. Temperatures generally range 200°C to 700°C depending on the reactor technology. Operating pressures may be ~2200 psi for pressurized water reactors. Molten salt environments are some of the most corrosive environment found in industrial processes. The large radiation fields further complicate the measurement through inducing unwanted electrical signals, altering material properties, and limiting the available material for sensor construction.

Qualifying a pressure sensor that covers all requirements and environments that may be encountered is challenging. Plenum pressure measurements are commonly desired in the range of 2 to 10 MPa, whereas pressure measurements in advanced reactors (helium/sodium/molten salt) only require pressures ranging from atmospheric to 2 MPa. This large dynamic range of pressures generally necessitates the use of different pressure sensors for each scenario. This combined with the material compatibility, time response, and temperature constraints establishes the need for qualifying a suite of pressure sensors.

Establishing and maintaining expertise and testing capability is required for the qualification of each sensor. This is especially true if the data will be used for nuclear fuel licensing or other safety basis measurements. This provides the motivation for the development of a versatile fiber-optic pressure sensor that can fit the needs for a variety of environments. The pressure sensor under development is based on Fabry-Perot interferometry using a diaphragm, which deflects under external pressure, as shown in Figure 1. This type of pressure sensor is commonly found throughout literature and some are commercially available. The existing developed sensors are not compatible with the temperature range, sensor size, pressure range, or the nuclear environment. However, there is no technical reason for these limitations.

Sensor Design

Fiber optic sensors have many inherent benefits that make them attractive for in-pile applications. These include their small footprint, electromagnetic immunity, high-temperature, high-speed sensing, and multi-modal capability. As with any classification of sensors, in-pile deployment comes with a unique set of challenges. For fiber optics, a common challenge is the radiation-induced attenuation. This can be mitigated through careful sensor design based on interference or phase measurements, rather than magnitude-based sensing. An example of this experimentally measured interference spectrum is shown in Figure 2. The cavity length, which provides a measurement of pressure based on the deflection of the diaphragm, is determined by the separation of adjacent peaks in the interference spectrum. The longer the cavity, the closer spaced the peaks are, and vice versa if

Continued on next page

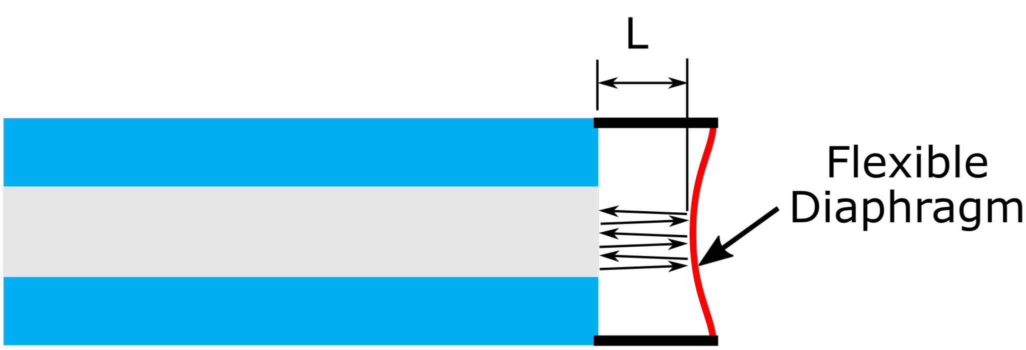

Figure 1. Diagram of a diaphragm-based extrinsic Fabry-Perot pressure sensor.

Continued from previous page

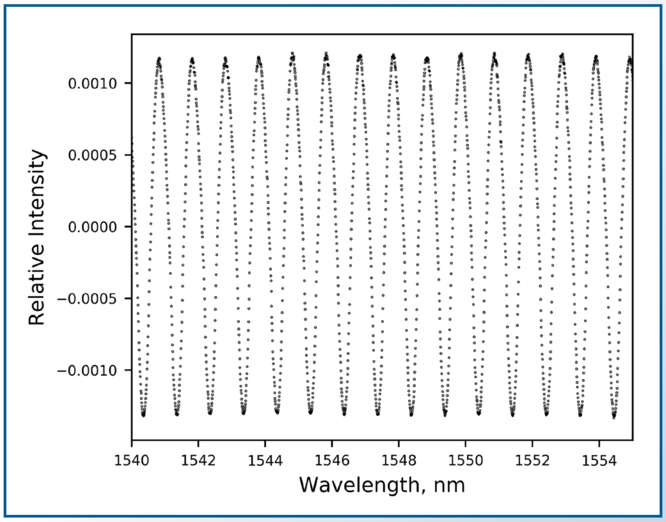

Figure 2. Measured interference spectrum from extrinsic Fabry Perot cavity.

the cavity decreases in length. As the signal decreases due to radiation induced attenuation the magnitude of these peaks decrease, but their separation is unaffected. Therefore, if enough light is transmitted that adjacent peaks can be identified, then the measurement can be conducted without a reduction in accuracy due to the attenuation.

This pressure sensor design can easily be modified for different pressure ranges through modification of the diaphragm geometry or material selection. By design, it is capable of pressure measurements in the kHz range for frequency response. The first iteration of the design is constructed from stainless steel that enhances its corrosion resistance and compatibility with most environments. The prototype, shown in Figure 3, can operate up to 350°C but planned improvements should extend continuous operation range to ~700°C.

Summary

This versatile pressure sensor under development and testing at Idaho National Laboratory can be customized for unique applications and is compatible with several near-term in-pile measurement requirements. This sensor has the potential to support the pressure measurement needs for a wide variety of advanced reactor needs and support continued in-pile testing of light-water reactor technology.

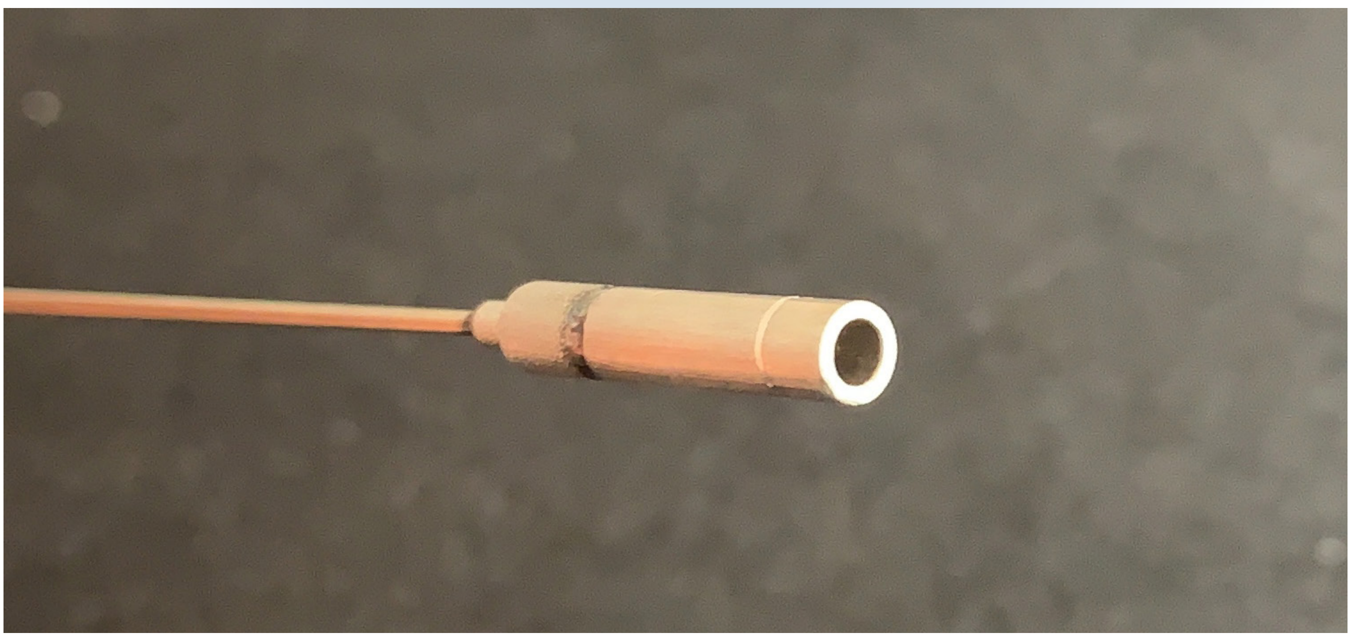

Figure 3. Image of prototype fiber optic pressure sensor.

Thermal Conductivity Needle Probe

Austin Fleming
Idaho National Laboratory

Kurt Davis
Idaho National Laboratory

Colby Jensen
Idaho National Laboratory

Introduction

Thermal properties of nuclear materials significantly impact the performance and safety analysis and operation of nuclear reactors. One of the most important properties is the thermal conductivity of UO2 fuel because it directly relates to how much heat can be extracted from the fuel. The thermal conductivity of UO2 is a complex function of burnup that can result in a significant degradation in the thermal conductivity of the lifetime of the fuel.

A variety of measurement techniques have been used to estimate thermal conductivity. These techniques include both measurements in post-irradiation examination and in-pile experiments. The experiments conducted in post-irradiation examination have generally used standard techniques, such as laser flash on a variety of samples, to capture the burnup dependence of thermal conductivity. [1] The Halden Reactor Project has used centerline thermocouples in the fuel to estimate the thermal conductivity. For this measurement, accurate knowledge of energy generated in the fuel rodlet, and the thermal hydraulic conditions must be known and well characterized. Uncertainty in gap conductance also presents challenges to this technique because of changing conditions from fuel swelling/gap closure.

The motivation for this work is to establish the capability to measure thermal conductivity in-pile without relying on detailed knowledge of the thermal hydraulic boundary conditions, heat generation, and gap conductance.

Sensor Design

Previously the approach taken for the thermal conductivity needle probe is based on the ASTM transient line source method. [2,3] A cross section of the sample and needle probe geometry can be seen in Figure 1. The probe is heated internally via joule heating in the heater wires, and the temperature response of the probe is recorded by a thermocouple. When the measurement is started, the probe and sample are at thermal equilibrium and a constant power is supplied to the heater wires causing a rise in temperature. At short-time scales after the heater is turned on, the thermal response of the system is dominated by the thermal properties and geometry of the probe. As time goes on, the thermal properties of the sample begin to dominate the thermal response.

The traditional transient line source technique measures the probe temperature during this heat-up phase. When the temperature is plotted against the logarithm of time, there is a linear region (constant slope) where this slope is proportional to the thermal conductivity of the sample. This linear region occurs on long-time scales where the probe can is considered to be a "line source" of heat. For this to be true, a significant amount of time is required, and the sample size must be sufficiently large that the heat does not reach the outer boundary condition of the sample. Otherwise, the linear region will not be established. Using this traditional method significantly limits the samples that can be measured.

Continued on next page

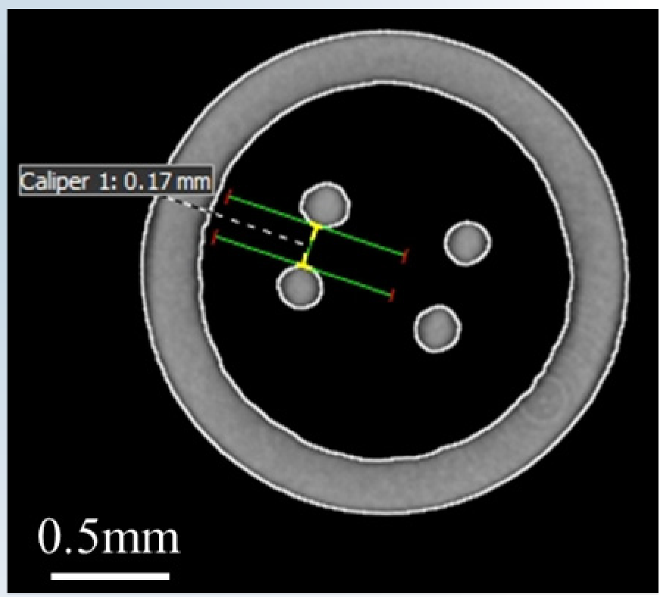

Figure 1. Cross section of the sample and needle probe geometry.

Continued from previous page

The development work at Idaho National Laboratory and Boise State University has established an analytic model based on a thermal quadrupoles approach to account for finite sample sizes, and a thermal contact resistance between the probe and sample. Through our collaboration, we compared this analytic model to detailed finite element analysis with excellent agreement. The method was then experimentally demonstrated using stainless steel and polytetrafluoroethylene (PTFE) samples of different radii and extracting thermal conductivity and contact resistance. The set of stainless steel samples were measured with and without thermal grease to demonstrate the method's resilience to changes in contact resistance. More detailed results on these findings can be found in published work in the International Journal of Thermal Sciences. [4]

Acknowledgements

We would like to thank Boise State University for their previous and on-going contributions to this work. Special thanks to Courtney Hollar, Katelyn Wada, and David Estrada.

References

[1] Ronchi, C., M. Sheindlin, D. Staicu, and M. Kinoshita, "Effect of burn-up on the thermal conductivity of uranium dioxide up to 100.000 MWdt—1," Journal of Nuclear Materials, Vol. 327, No. 1, pp. 58–76, 2004, doi: 10.1016/j.jnucmat.2004.01.018.

[2] ASTM, "Standard test method for thermal conductivity of plastics by means of a transient line-source technique," 2001 Annual book of ASTM standards, Vol. 8, pp. 699–703, 2001.

[3] ASTM, "Standard test method for determination of thermal conductivity of soil and soft rock by thermal needle probe procedure," ASTM Data Ser. Publ., Vol. 5334, pp. 1–8, 2008.

[4] Hollar, C., A. Fleming, K. Davis, R. Budwig, C. Jensen, and D. Estrada, "A parametric study for in-pile use of the thermal conductivity needle probe using a transient, multilayered analytical model," International Journal of Thermal Sciences, Vol. 145, p. 106028, 2019, doi: 10.1016/j.ijthermalsci.2019.106028.

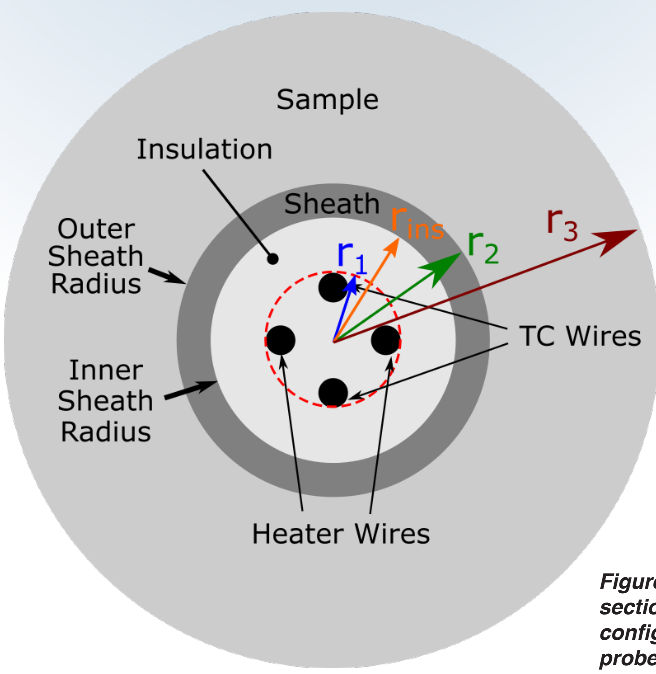

Figure 2. Diagram of the cross section of the experimental configuration showing the needle probe internals at the center.

Resonant Ultrasound Spectroscopy for In-Pile Microstructure Monitoring

Robert Schley
Idaho National Laboratory

David Hurley
Idaho National Laboratory

In pile monitoring of microstructure evolution of nuclear fuels and materials will enable an enhanced understanding of the effects of radiation on material performance. It would also enable monitoring in pile material properties that cannot be captured in a post-irradiation environment. This has motivated the development of facilities that combine ion beam irradiation with transmission electron microscopy. However, creating neutron beams that have a flux and energy distribution representative of in pile conditions is currently not possible; thus, a comparable capability to examine the influence of neutron irradiation on microstructure evolution does not currently exist. To close this capability gap will require development of innovative instruments that can indirectly measure changes in microstructure. The work presented here describes the development of an in pile laser resonant ultrasound spectroscopy instrument to measure changes in elastic properties that can be tied directly to changes in microstructure.

Methodology

Our approach for in-pile monitoring of microstructure consists of tracking the change in resonant frequency of a vibrating beam fabricated from the material of interest. [1]

Changes in microstructure can have a pronounced influence on elastic properties. Examples include grain restructuring, gas bubble formation, and void swelling. The changing elastic properties can be measured by monitoring the resonant frequency, which depends only on the beam geometry, density, and the elastic properties. Free free beams are generally specified for these types of measurements as the influence of the environment can be minimized; however, cantilever beams offer advantages for in-reactor measurements because the beams can be held rigidly in position and alignment with the detection system can be maintained.

Excitation and detection of the beam vibrations are accomplished using optical techniques. An amplitude modulated laser serves as the excitation source and an optical knife edge technique using broadband white light is used for detection. Optical fibers are used to transmit the excitation and detection light to and from the sample eliminating the need for sensors or detectors in the reactor environment.

Accomplishments

An irradiation instrument capsule for use with a cantilever beam, as shown in Figure 1, was developed and tested during the 2019 fiscal year. Thermally driven grain restructuring (recrystallization) of a highly textured copper sample under irradiation was studied. Several beams for testing were cut from a rolled copper sample using electrical discharge machining. Using the instrument capsule, laboratory tests were run at 150,

Continued on next page

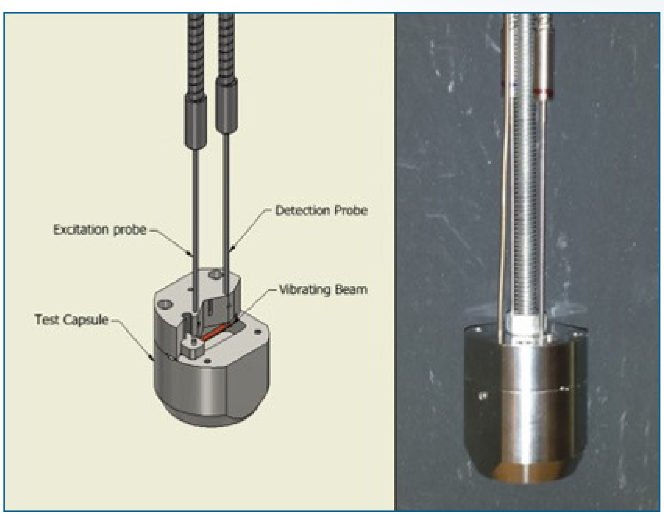

Figure 1. Section view of the test capsule showing the cantilever beam with excitation and detection probes (left), capsule prior to reactor test (right).

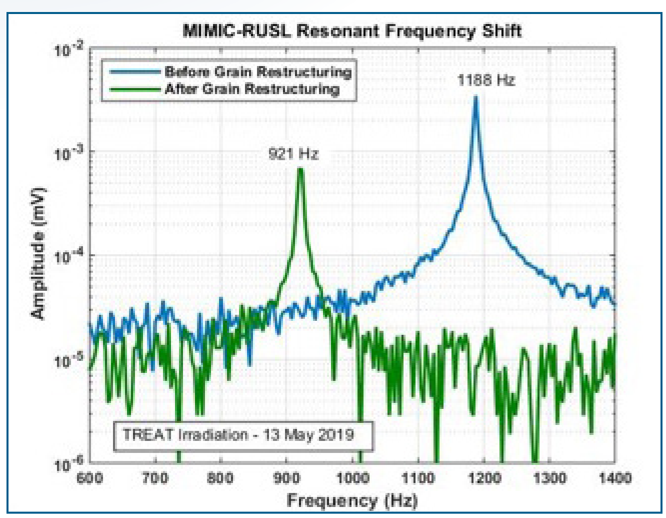

Figure 2. Resonant frequency before and after grain restructuring.

Continued from previous page

160, 170, and 230°C to determine the time required for the recrystallization process at each temperature. An irradiation test was then conducted at the Idaho National Laboratory's Transient Reactor Test (TREAT) facility. The reactor was run in steady state mode at 80 kW. After reactor startup, the experiment was heated to 160°C and held at that temperature for 4 hours while continuously monitoring the resonant frequency of the vibrating sample. During the grain restructuring process, the resonant frequency of the beam transitioned from 1,188 Hz to 921 Hz, as shown in Figure 2. The resonant frequency transition of the beams at 160°C from the laboratory tests and the irradiation test were then compared to determine the impact of the irradiation on the recrystallization. The results indicated little difference between the two tests. This is in agreement with previous scoping studies that indicated that at the dose rate provided by TREAT, radiation enhanced diffusion would not bring about a significant reduction in the recrystallization temperature. [2] However, this experiment provides an important baseline for future studies using uranium-based fuels.

Current Work

Current work is expanding on the success of the irradiation test conducted last year by developing a similar instrument capsule that uses a free-free beam.

While a cantilever beam offers the advantage of a rigidly held beam and large displacements, the cantilever boundary condition can be extremely difficult to realize and correction factors are required to approximate the elastic constants. In addition, future studies that consider using acoustic attenuation to characterize microstructure will be severely impacted by acoustic coupling to the environment through the cantilever end. Designs for an instrument capsule that allow vibration of a free beam while minimizing translation of the beam are being developed and evaluated. Figure 3 shows initial testing of a free beam capsule concept. Methods of validation and verification of microstructure characterization based on advanced modelling and simulation are also part of the current work scope.

References

[1] Schley, R. S., D. H. Hurley, Z. Hua, "Optical fiber technique for in-reactor mechanical properties measurement," AIP Conference Proceedings, Denver, Colorado, July 15–20, 2012, 1511, pp. 1701–1709, 2013.

[2] Schley, R. S., L. K. Aagesen, Z. Hua, Detailed Analysis of RUS Insertion Experiment and Scoping Studies for Performing Next Experiment using an Enriched Fuel Sample, Idaho National Laboratory, INL/EXT-19-55962, September 2019.

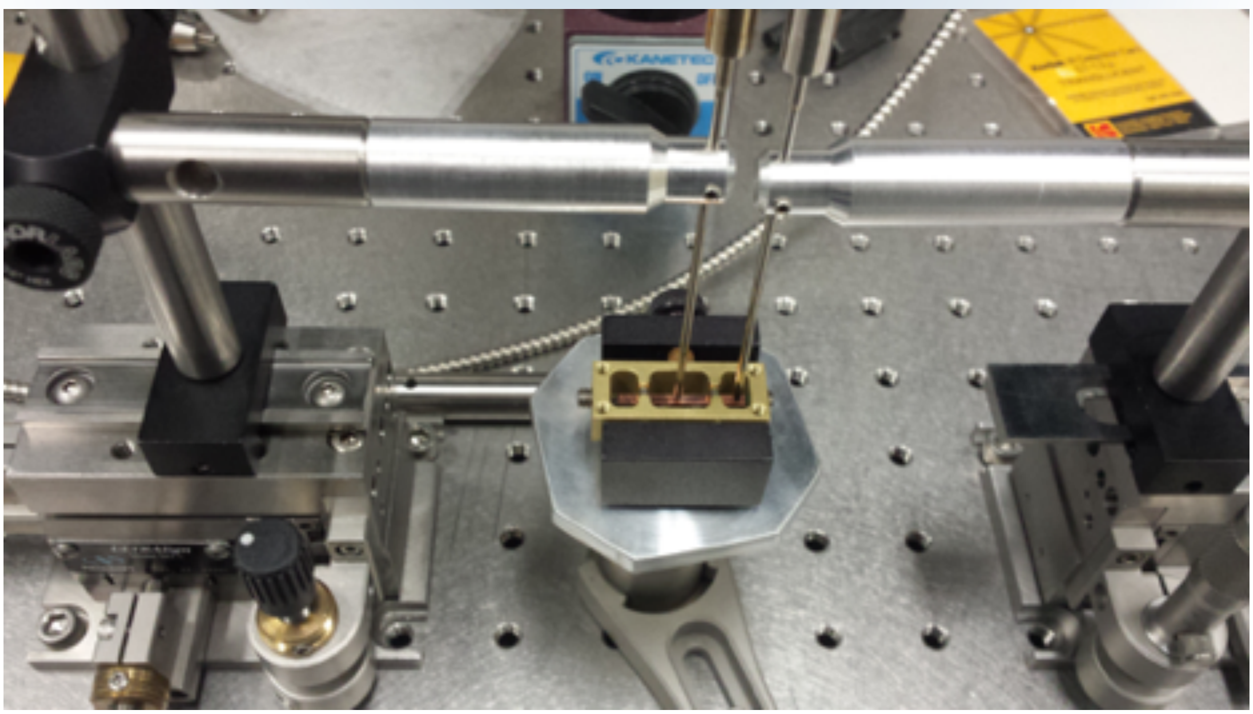

Figure 3. Initial testing of a free beam instrument capsule concept.

Development of an Electrochemical Impedance Instrument for In-pile Monitoring Cladding Materials Behaviors

Hongqiang Hu
Idaho National Laboratory

Michael F. Hurley
Boise State University

Hui Xiong
Boise State University

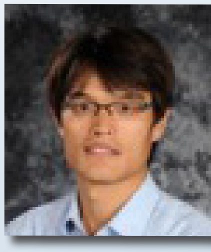

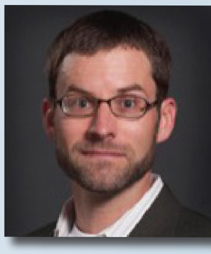

The ability to probe local structural/ chemical changes at critical locations is a grand challenge in current nuclear power plants. The challenge arises from the unique combination of temperature, irradiation, corrosion, and space restriction, to which the conventional methods cannot be applied. These harsh and complex environments in nuclear reactors make research necessary to correlate material performance with evolving microstructure and then develop and deploy unique instruments to characterize the behavior of fuels and materials during irradiation tests. The In-Pile Instrumentation Initiative (I2) under the Department of Energy's Office of Nuclear Energy's (NE) Advanced Sensors and Instrumentation program is conducting these kinds of research with a vision to provide real-time, accurate, spatially resolved information regarding performance of fuels and materials that can be directly tied to microstructure.

Project Objectives and Goals

This project's objective is to prove that the electrochemical impedance spectroscopy (EIS) technique can be applied to study the non-stoichiometry, microstructure change and corrosion mechanisms of cladding materials at high temperatures. This will eventually lead to develop an integrated real-time sensing technology for in-pile monitoring of changes in cladding materials by coupling it with model simulation and material characterization. [1] This project will involve the initial development of electrochemical sensing technologies for measuring spatial and time resolved changes in cladding chemistry. Specific attention will be paid to monitoring changes in cladding hydride formation and deformation, and cladding corrosion. At the end of the project, in-pile testing in an irradiation environment will be designed and assessed.

Technology Approach

This project is a collaborative effort among researchers based upon strong interdisciplinary scientific collaboration including electrochemical process, material characterization, and finite element (FE) modeling. EIS signals are collected from experiments on cladding materials, then equivalent circuit models are established, from which process parameters are obtained. These results are applied for interpreting the compositional and structural evolutions of cladding materials through the change of impedance response (resistance and capacitance) at certain frequencies.

Continued on next page

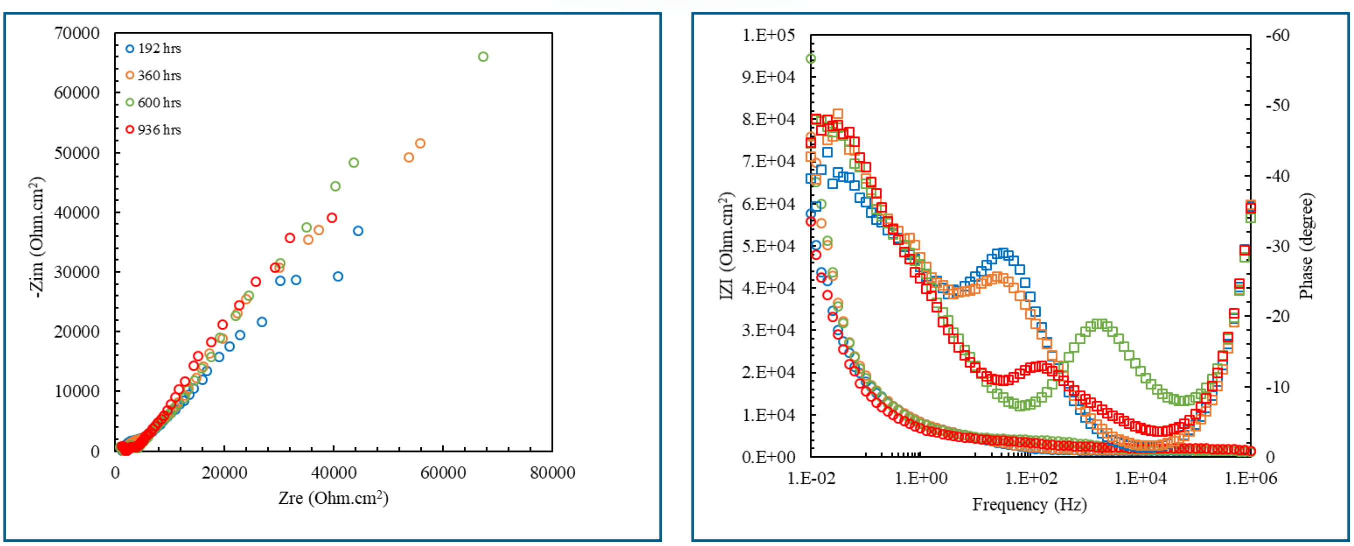

Figure 1. Impedance spectra for sample Zr-4 as a function of immersion time: left for Nyquist and right for Bode plot.

Continued from previous page

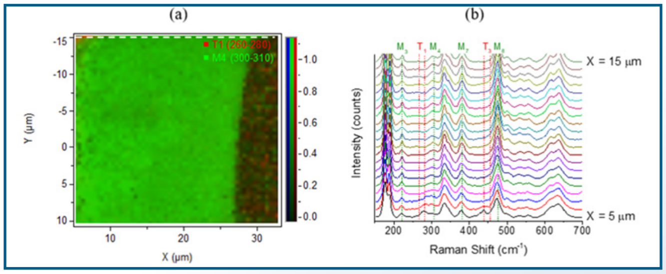

Figure 2. Ramen mapping for Zr alloy: (a) Co localized mixed intensity maps presenting tetragonal, T1 (red) and monoclinic, M4 (green) peaks. (b) Waterfall of Raman spectra near the metal/oxide interface, corresponding to the dotted line in the mixed intensity map.

Advanced material characterization includes scanning electron microscopy and tomography characterization of delayed hydride cracking and associated mechanisms, as well as visualization of microstructure evolution, synchrotron characterization of the structure of cladding hydride, and Raman spectroscopic characterization of hydrogen evolution on surface at elevated temperatures. Characterization results are used to verify and validate EIS data and models.

An FE modeling framework is developing based on the BISON and an FE fuel performance code, and applied the model to one selected Zircaloy-4 cladding that is designed for less hydrogen uptake in certain reactor conditions. The model is composed of three sections of physics processes: heat conduction, mechanical deformation, and hydride evolutions. [2] The FE code as well as microscopic identification of defects and transport carriers will be used to help interpret the experimental EIS data.

Progress and Results

Extensive research efforts have been made and good progress has been achieved on this project, which resulted in several publication. Two peer-reviewed papers are published, a review journal paper is ready for submission, and two more manuscripts are under preparation with good results.

Two EIS testing systems were designed: one is for air-environment for investigating both fuel pellets and cladding materials; another is for aqueous conditions for cladding materials only. The impedance spectra for a sample Zr-4 as a function of immersion time is demonstrated in Figure 1, which provides information about its structural changes. If a dense oxide is formed, one time constant is sufficient to model the impedance data. The frequency dispersion commonly observed could be attributed to surface roughness of the underlying metal and dielectric relaxation. [1,2] If the oxide is composed of multiple layeres with different properties, several time constants are needed to model the data. The changes in properties are resulted from changes in the pore structure.

High-temperature, in-situ Raman provides observation of oxidation stress at the surface of the oxide. A transition from tetragonal to monoclinic zirconia can be seen early in the oxidation experiment as demonstrated in Figure 2, which is induced by massive shifts in stress as the oxide grows. [3] In addition, atom probe tomography (APT) has supplied evident differences in the distribution of zirconium and oxygen at the metal/oxide interface. All metal/oxide parameters are summarized schematically in Figure 3. The percent tetragonality, stress, Volta potential, and oxygen concentration are shown for different phases of zirconia and zirconium metal. [4]

Preliminary results of FE modeling on hydride evolution and distribution showed that the hydrogen concentration can penetrate the cladding/coolant surfaces and reach a depth of 0.5 mm during 1-year evolution, and most of the hydrogen stays near the cladding/coolant surface Figure 4. [2]

Continued on next page

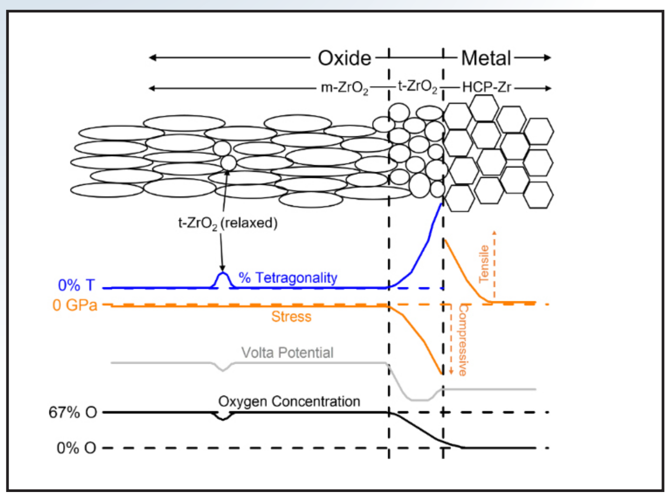

Figure 3. Schematic summarizing the different parameters for each zirconia and zirconium phase.

Continued from previous page

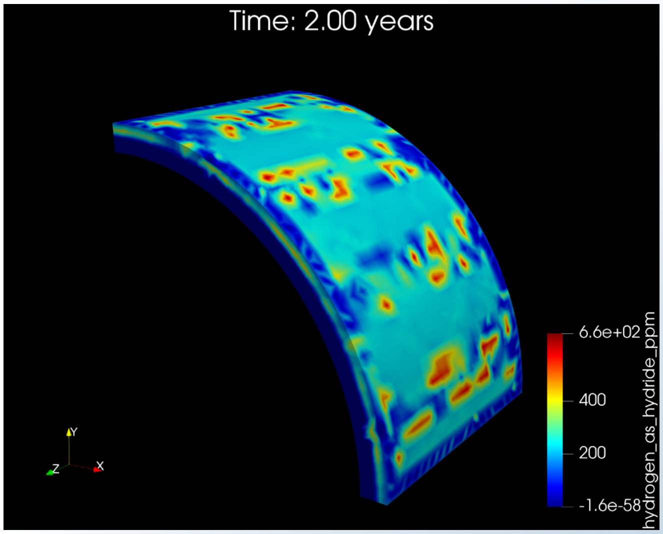

Figure 4. FE simulations of hydride evolution

Impact and Value to Nuclear Applications

This electrochemical study mainly focused on the impedance technique for cladding material characterization in a high-temperature water environment. Upon successful completion, the most important contribution of this project is the establishment and proof of EIS technique and demonstration of the in-situ EIS measurement of cladding materials under the condition of pressurized primary coolant. Impedance spectroscopy is an efficient and nondestructive tool to characterize the electrical response of a particulate system, and it is also very sensitive to changes that might have an influence on the electrical properties, which conventional techniques would have difficulty observing. Hence, an in-situ EIS-based sensor can provide real-time information for in-pile monitoring of changes in cladding materials without interrupting the reactor operation. In addition, with the knowledge gained from this project, in parallel with research from others, a thorough understanding of the zirconium corrosion system can be achieved. By further applying this knowledge to developing better materials, an improved performance of the new alloy would be expected.

Plan Forward

Future work will focus on the design and testing of the EIS sensor at pressurized water reactor-relevant conditions in static and flowing autoclave in order to investigate the effects of various environmental conditions (temperature and pressure) on cladding material corrosion mechanism. The FE model will be finalized, and EIS spectra of hydride and its correlation with characterization features will be analyzed.

References

[1] Hu, H., C. Efaw, M. Reynolds, M. Hurley, C. Xiong, Development of an Electrochemical Impedance Instrument for Monitoring Corrosion Formation (Oxide and Hydride) on Cladding Materials, Idaho National Laboratory, INL/LTD-19-53207, 2019.

[2] Hu, H., L. Ding, C. Efaw, M. Reynolds, M. Hurley, C. Xiong, M. Long. Design of Impedance Based Sensors for Monitoring Corrosion Formation of Cladding Materials, Idaho National Laboratory, INL/EXT 19 55956, 2019.

[3] Efaw, C. M., J. L.Vandegrift, M. Reynolds, S. McMurdie, B. J. Jaques, H. Hu, H. Xiong, M. F. Hurley, "Characterization of Zirconium Oxides Part I: Raman Mapping and Spectral Feature Analysis," Nuclear Materials & Energy, December 2019, Vol. 21, 100707.

[4] Efaw, C. M., J. L.Vandegrift, M. Reynolds, S. McMurdie, B. J. Jaques, H. Hu, H. Xiong, M. F. Hurley, "Characterization of Zirconium Oxides Part II: New Insights on the Growth of Zirconia Revealed Through Complementary High-Resolution Mapping Techniques," Accepted at Corrosion Science, January 2020.

In-Pile Instrumentation: Printed Melt-Wire Chips for Cheaper, Compact Instrumentation

Kunal Mondal
Idaho National Laboratory

Kiyo Fujimoto
Idaho National Laboratory

Michael McMurtrey
Idaho National Laboratory

Introduction

The harsh environment within a nuclear reactor introduces unique challenges to materials such as fuels and structural components as they are required to withstand intense irradiation, high-operating temperature, large stress/strain, etc. To develop a better understanding for the effect of this environment on these components, these materials must undergo rigorous testing to evaluate their performance under reactor conditions. Of particular interest is the effect of neutrons, which is unique to the nuclear field. The ability to investigate the neutron response of a material is facilitated by materials test reactors, such as the Advanced Test Reactor (ATR) at Idaho National Laboratory (INL). While some experiments need only to study the material with post-irradiation examination to complete their research objectives, others require reliable data collection inside the reactor during the irradiation. As a result, significant efforts towards research and development in sensors and instrumentation have provided tremendous advancements in the availability and reliability of instrumentation for irradiation tests in materials test reactors.

The Advanced Manufacturing portion of the In-Pile Instrumentation program has been exploring novel technologies that would allow for the development of unique sensors that are not possible through conventional fabrication processes. The direct-write techniques of aerosol jet printing and plasma jet printing were identified as tools with significant promise in diversity of application to produce wide-range sensors that are not only miniature, but also robust. For nuclear instrumentation, these benefits are extremely advantageous. Aerosol jet printing and plasma jet printing are capable of creating complex 2D designs while utilizing an ever-growing list of materials, and these benefits provide significant potential for the development of innovative in-pile instrumentation. Similar to printing documents with more familiar computer ink-jet printers where the inks contain dyes for paper, the inks used in aerosol jet printing and plasma jet printing contain nanoparticles of metals and/or ceramics. These inks can then be used to form narrow (anywhere from tens to hundreds of micrometers wide) and thin (typically hundreds of nanometers thick) lines in an arrangement as designed by the researcher. For the print to be functional, it is sintered, which then creates wires and films. These wires and films, when properly arranged, act as active or passive sensors. Active sensors, such as strain gauges, send a feedback signal that reports the state of the sensor during the test in real-time. Passive sensors, such as dosimeters, send no signal, but are examined after the test to determine characteristics of the prior experiment conditions. While in many cases active sensors are considered superior to passive sensors in terms of quantity of data, passive sensors may often be preferred as they can easily be added to any experiment. This ease is provided by the fact that they do not require feedthroughs and are often relatively cheap.

Continued on next page

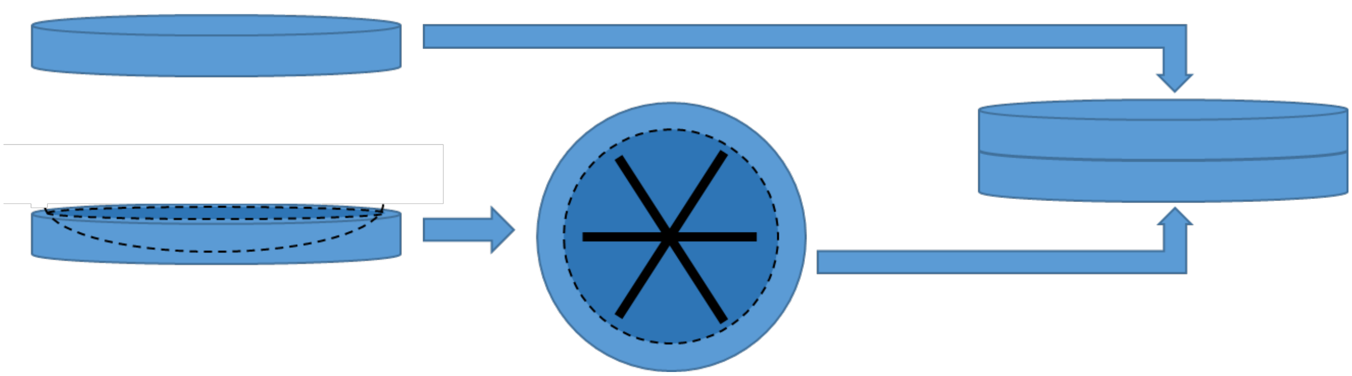

Figure 1. Schematic illustrating the staggery for the melt wire printing and encapsulation.

Continued from previous page

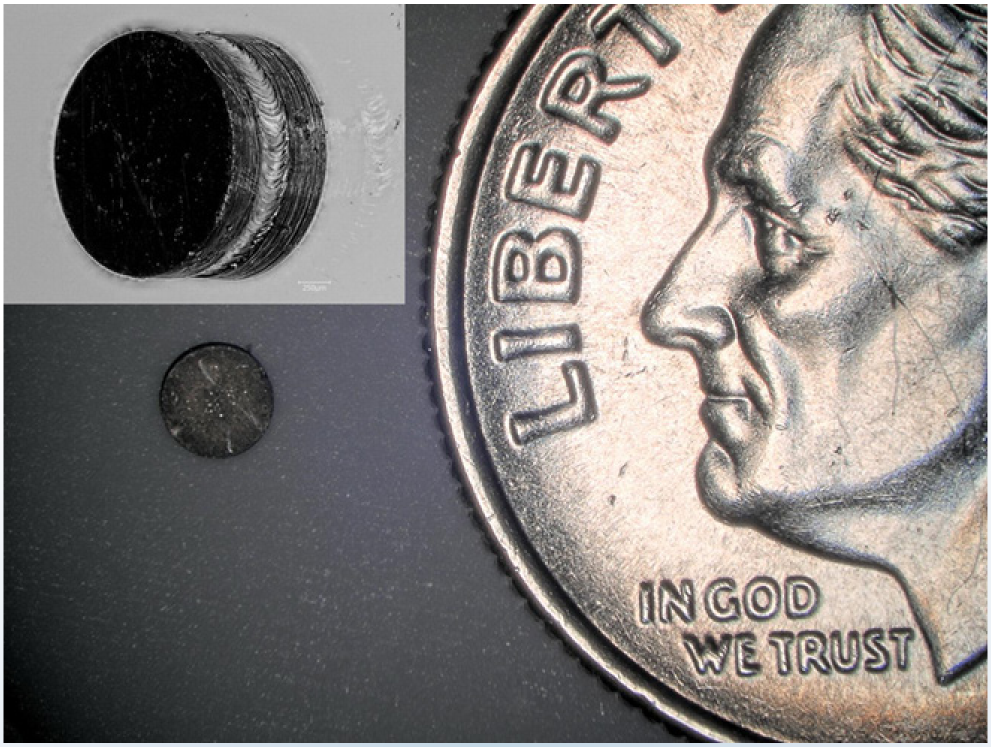

Figure 2. 2-mm-diameter melt wire sensor chip alongside a dime. The inset shows clear view of laser welded chip.

Simple sensors for complex problems

Melt wires are a passive sensor used to determine peak temperatures during an irradiation test. Metal wires are created from materials having well-known compositions and melting temperatures. For irradiation testing purposes they are positioned within the reactor to characterize the environment during the test. Once testing has been completed, the wires undergo visual inspection to investigate whether the melting point of the melt wire material has been achieved. This information allows the researcher to determine that the maximum peak temperature was greater than the melting point of those melt wires that did melt, and lower than that of those that did not melt. Traditional melt wires are commonly used test reactor experiments such as ATR. [1-2] However, analysis is highly subjective, and some test designs simply do not have the space for traditional melt wires. Test capsules that are only a couple millimeters in diameter while also being packed with specimens do not have the space for the wire filaments that are traditionally encapsulated in quartz.

To address this challenge of having very limited space, novel melt wire designs were required. For this, a melt wire "chip" was designed with a schematic of this design provided in Figure 1. A two millimeter diameter stainless steel disk that was half a millimeter thick was milled to create a dimple or pocket. Melt wires were then printed within the pocket using one of the direct ink writing techniques (each melt wire may be of a different composition to provide a range of potential melting temperatures). Utilizing a laser welder, a second steel disk was then welded overtop. This created a melt wire chip, which is shown in Figure 2. With this design, a two-fold benefit is observed as melt wires can now be easily placed within an experiment having very small size requirements, and concerns towards the environment they are exposed to can be reduced, as the wires are now sealed within the steel.

While the sealed disks protect the metal wires from corrosive test environments, they expose limitations in traditional methods used for visual inspection. To

Continued on next page

Continued from previous page

overcome this, X-ray computed tomography (CT) was used to inspect the melt behavior of the sealed wire. To validate the melt behavior of the printed melt wires, initial testing was performed in a furnace with a chip containing a printed silver wire. It was heated to 1,000°C to ensure that the silver wire would melt and was imaged using X-ray CT before and after melting, as shown in Figure 3. The wire deformed and material appeared to have migrated after melting, which is visible with the X-ray CT image.

Summary and conclusions

INL has enhanced its melt wire capabilities with the introduction of advanced manufacturing techniques. It has been demonstrated that utilizing these techniques enable the support of irradiation testing within ATR and other test reactors having significant space limitations. With the use of direct-write techniques, a peak temperature sensor has been fabricated that is two millimeters in diameter and one millimeter thick. A noteworthy benefit of these chips associated with miniaturization of the melt wire is the ability for one chip to contain multiple melt wires having different compositions. Furthermore, encapsulation of the melt wires provides protection from potentially corrosive environments, and X-ray CT allows for visualization of the melt wires to determine the peak temperature of the reactor during an experiment. Initial testing has been performed outside of the test reactors to validate not only the manufacturing procedure, but also the ability to visualize the melted wires. The first insertion of a melt wire chip into a test reactor is expected to occur in the fall of 2020.

References

[1] Davis, K. L., D.L. Knudson, J. E. Daw, J. L.Rempe and A. J. Palmer, "Melt Wire Sensors Available to Determine Peak Temperatures in ATR Irradiation Testing," 8th International Topical Meeting on Nuclear Plant Instrumentation, Control, and Human Machine Interface Technologies (NPIC&HMIT2012), San Diego, California, July 22–26, 2012.

[2] Rempe, L., D. L. Knudson, J. E. Daw, T. C. Unruh, B. M. Chase, K. L. Davis, A. J. Palmer, and R. S. Schley, "Advanced in-pile instrumentation for material and test reactors," in 2013 3rd International Conference on Advancements in Nuclear Instrumentation Measurement Methods and their Applications (ANIMMA), 2013, pp. 1–11, DOI: 10.1109/ANIMMA.2013.6728013.

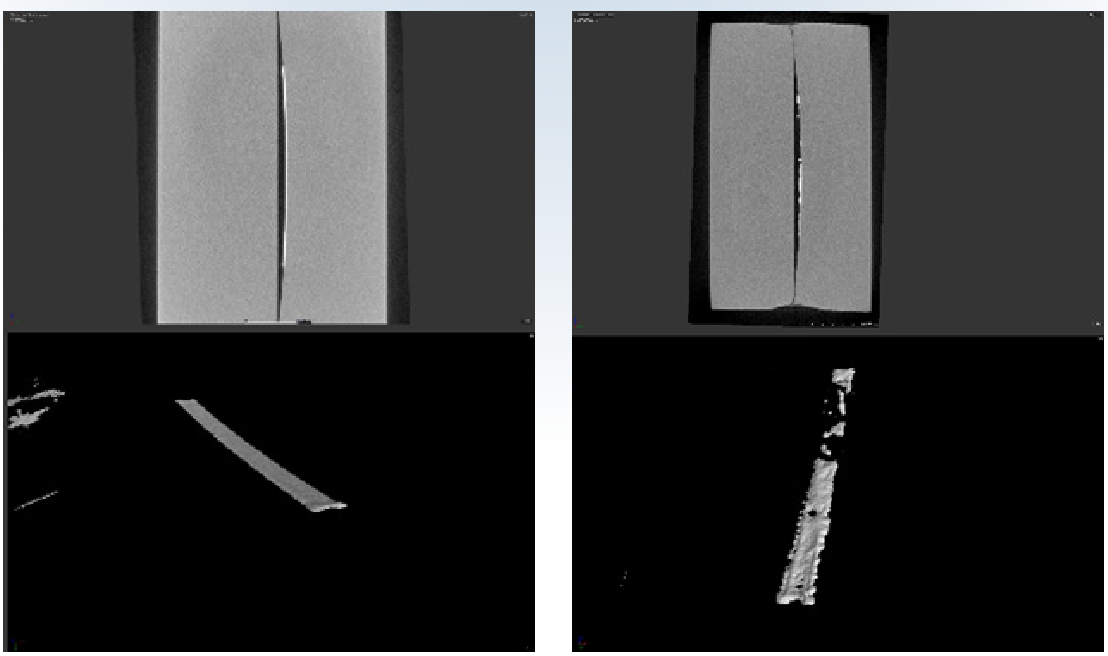

Figure 3. X-ray CT scan of the melt wires (left) before heating, and (right) after heating to 1000°C inside a furnace. The upper images show a cross section of the entire chip, and the lower images show just the meltwire.

Flowing Autoclave System

Richard Skifton
Idaho National Laboratory

Introduction

Idaho National Laboratory's out-of-pile, flowing autoclave system (FAS) provides fast turnaround testing and active monitoring of instrumentation. The FAS is capable of testing at pressurized water reactor conditions prior to irradiation in the Advanced Test Reactor (ATR), or similar materials test reactor. Effects of high-temperature, high-pressure, water chemistry, and flow induced vibrations can be tested on the following types of sensors:

- Temperature
- Fluence (neutron)
- Dimensional
- Loop Pressure
- Water Chemistry
- Crack Growth Rate
- Thermal Conductivity
- Gamma Heating
- Fission Gas
- Loop Flowrate
- Crud Deposition
- and more…

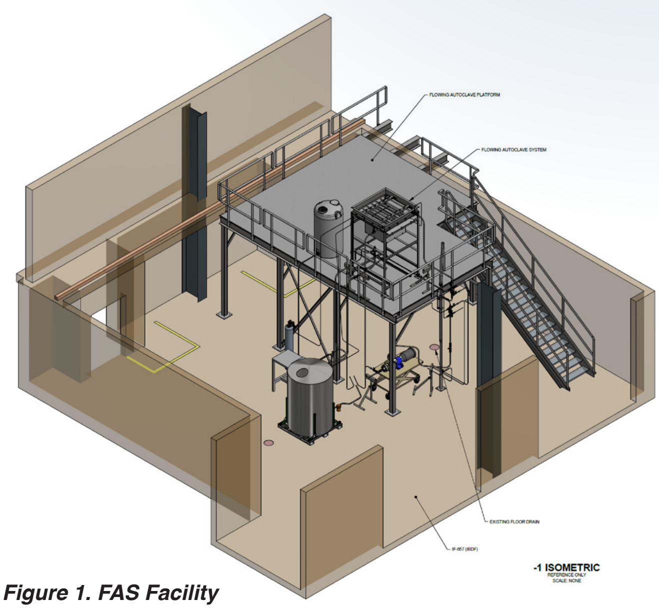

Figure 1. FAS Facility (Isometric View). For Information Only. High bay overhead crane not shown.

FAS Facility

The FAS facility is located at the Idaho National Laboratory's Engineering Demonstration Facility. The facility accommodations include:

- High Bay
- Overhead Crane
- Mezzanine Access
- Various Loops
- Control Room
- Data Acquisition Suite
- Deionized Water System
- Chemical Composition

The high-bay access doors and ceiling with accompanying overhead crane allows for horizontal-to-vertical insertion of prototypic test trains into the FAS loop. Figure 1 shows the complete water loop with supporting mezzanine.

ATR Relevancy of FAS Loop

The FAS water loop can achieve temperatures and pressures above and beyond standard commercial pressurized water reactors. Thus, providing a 1:1 comparison between FAS and ATR water loops, allowing for true pre-irradiation sensor effects testing. FAS has relevant test sections that match several irradiation positions in the ATR and other material test reactors.

Matching FAS test sections to various irradiation positions within the ATR are governed mainly by three factors: cross-sectional area, desired neutron flux, and relative availability (schedule). Three main irradiation positions accommodate the approximate mid-range of all three criteria: the small-I, medium-I, and large-B positions (highlighted in red in Figure 2).

Table 1. Achievable parameters of FAS.

Parameter		Measurement
Flow Rate		50 gal/min
Temperature		320°C
Pressure		2800 psi
Water Chemistry		Yes, Controlled
Test Sections Available	Length	40 in.
	Diameter	1 in. & 1.5 in.

Continued on next page

Continued from previous page

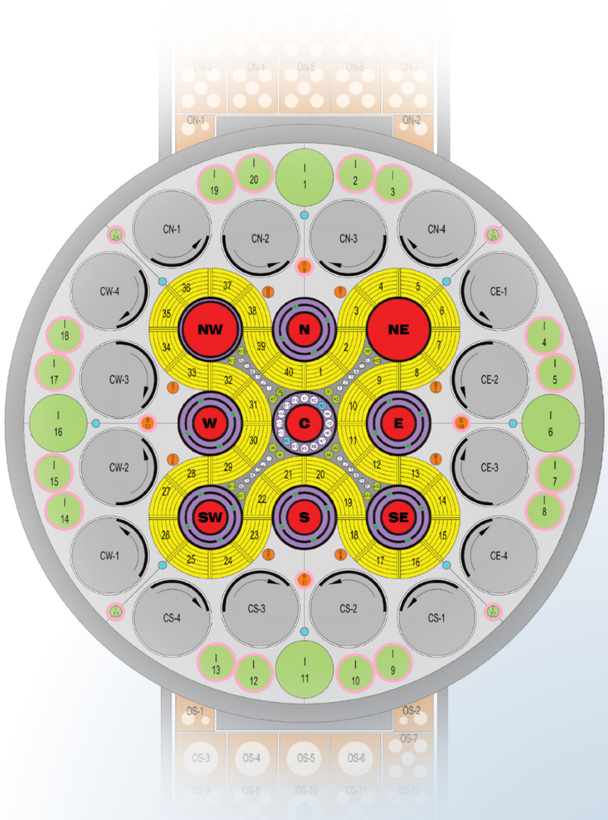

Figure 2. ATR core cross section with irradiation positions relevant to the FAS highlighted in red.

The diameter, average thermal and fast flux of these positions are shown in Table 1.

Table 2. Achievable metrics of FAS relevant test sections inside the ATR.

Position	Inside Diameter (Effective) [in]	Thermal Flux [n/cm2-s]	Fast Flux (E>1 MeV) [n/cm2-s]
Small-I	1.5	8.4×10^{13}	3.2×10^{12}
Med-I	3.5 (1.5)	3.4×10^{13}	1.3×10^{12}
Large-B	1.5	1.1×10^{14}	1.6×10^{13}

The medium-I position, specifically the I-9 position in the southeast corner, has an effective diameter of 1.5 in. due to various tubing and sensor leads that need to be inserted in order to operate. This is the main reason for FAS test sections have an equivalent 1.5-in. inside diameter.

FAS Schedule

To discuss or schedule work in the FAS loop please contact:

Dr. Richard Skifton
208.526.2696 | Richard.Skifton@inl.gov

CURRENT PROJECTS PLANNED TO BE TESTED IN THE FAS LOOP FOR FY 2020

<table>
<tr><th>March</th><th>April</th><th>May</th><th>June</th><th>July</th><th>August</th><th>September</th></tr>
<tr><td colspan="3">Optimized design of the High-Temperature Irradiation-Resistant Thermocouples (HTIR-TC)</td><td></td><td></td><td></td><td></td></tr>
<tr><td></td><td></td><td colspan="3">Linear Variable Differential Transformer, stressed and unstressed
• Creep Test Rig
• Constant Velocity Diameter Gauge.</td><td></td><td></td></tr>
<tr><td></td><td></td><td></td><td></td><td colspan="3">Ultrasonic Thermometers (UTs)</td></tr>
</table>

Noninvasive High Temperature Embedded/Integrated Sensors (HiTEIS) for Remote Monitoring of Nuclear Power Plants

Howuk Kim
North Carolina State University

Kerrigan Sean
North Carolina State University

Bharat Balagopal
North Carolina State University

Mo-Yuen Chow
North Carolina State University

Mohamed Bourham
North Carolina State University

Xiaoning Jiang
North Carolina State University






Introduction

Reliable sensing is crucial to ensure the safety and functionality of nuclear power plants (NPPs). Most conventional NPP sensors perform in an invasive manner, contacting with the internal media. [1] The typical invasive sensors are prone to damage in harsh environments, and most sensors have degraded reliability in the long period of usage, which may result in frequent sensor maintenances and the regular shutdown of the plant. [2] Moreover, calibration and maintenance of invasive sensors and detectors usually expose human technicians to radiation conditions. [3]

Noninvasive sensors enable monitoring of structural integrity and plant operation status without affecting the structure and internal media. Furthermore, noninvasive sensing would provide a much more economical option for sensor calibration and maintenance. Combining with the nonintrusive sensing technique, wireless data-transfer technologies may further reduce the possibility of human dangers and enhance the cost-effectiveness of plant operation since the operation status of an NPP can be monitored from a remote and safe place. Despite many potential advantages of the noninvasive sensing technique, there has been a lack of non-invasive sensor investigations for the NPP applications. One challenge might be the fact that sensors applied in NPP structures may face harsh environmental conditions including high temperatures (HT) and irradiation in NPP structures. [4] As such, it is essential to employ proper sensing materials, as well as, sensing mechanisms. For the last decades, there have significant advancements in sensor materials robustness to such environmental conditions. For instance, non-ferroelectric piezoelectric single crystals, such as Lithium Niobite, Yttrium Calcium Oxoborate, and Aluminum Nitride (AlN), can operate stably at a relatively HT condition (~1,000°C) without any phase transition. [5-6] Furthermore, among existing HT single crystal materials, AlN is known for its robust sensing performance under radiation conditions involving neutron and gamma fluence. [7]

The goal of our research is to develop noninvasive high-temperature embedded/integrated sensors (HiTEIS) for remote monitoring of NPPs Figure 1. This article presents the current research status of the noninvasive HiTEIS techniques and the wireless communication system, followed by the introduction of potential future work.

Noninvasive HiTEIS

In this project, various noninvasive sensing methods were investigated to measure vibration, stress, and liquid level, and to detect structure damages. These noninvasive sensors can basically operate at the outer surface of a structure as illustrated in Figure 1. Piezoelectric materials were used in these sensors because of the fast response and simple structure design of piezoelectric sensors. Moreover, acoustic sensors are known with excellent wave penetration into a metallic structure, and the cost effectiveness make them preferable for the noninvasive sensors.

1. **Vibration sensor.** The vibration sensor measures a vibration level of a structure using the direct piezoelectric effect, where the vibration-induced inertial force acting on the piezoelectric element results in an electrical charge or voltage output. For the HT application, AlN piezoelectric single crystal was employed. In addition, platinum foils (a thickness of 1

Continued on next page

Continued from previous page

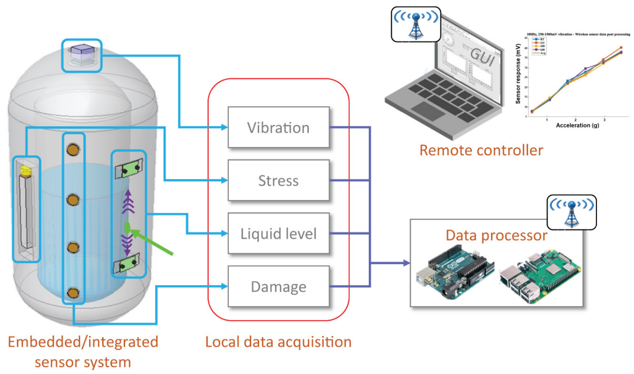

Figure 1. Overview of HiTEIS with the wireless data communication.

μm) and platinum wires (a diameter of about 100 μm) were integrated with the active elements between the base structure and the seismic masses. The sensor performance was validated under HT condition up to 1,000°C. The sensitivity of the sensor was less influenced by temperature variation. Furthermore, the radiation resistance of the sensor was validated by measuring the sensitivity change between the pre- and post-exposure of gamma radiation with a total dose of 11 kGy.

2. **Stress sensor.** The stress sensor is capable of noninvasively measuring either pressure inside a pressurized vessel or stress in the vessel wall. The sensor made use of the acoustoelastic effect, which assumes that stress level has an influence on the wave velocity as well as the time-of-flight. Two different types of wave-generating methods were considered in our research: (1) contact wave generation using a piezoelectric composite transducer and (2) noncontact wave generation using a pulsed laser Figure 3(a). The stress level of a pressurized vessel was measured using the time-delay of a subsurface longitudinal wave signal. Figure 3(b) demonstrates that the laser-generated ultrasound wave signal is linearly delayed with respect to the mechanical stress level.

3. **Liquid level sensor.** The liquid level sensor noninvasively measures fluidic level inside a metallic vessel, as shown in Figure 4. The sensor measured liquid level was based on leaky guided ultrasound waves where it was assumed that the wave intensity correlates with the dissipation of liquid media. The ultrasound wave was generated using a pulsed laser from a remote place. The guided ultrasound wave was received at two AlN sensing elements, embedded in the test structure. A mathematical expression on the liquid level index was introduced to quantify the liquid level from measured wave signals. The HT sensing was validated using oil media at up to 200°C.

4. **Damage detector.** An HT damage detection sensor was investigated using a laser ultrasound transmitter and a piezoelectric receiver Figure 5. While noncontact transducers are capable of transmitting and receiving ultrasound waves from a remote place, the low signal-to-noise ratio and the low-sensitivity limit the practical application of the sensor. In our study, we compromise the receiving unit by employing a contact type piezoelectric sensor. AlN single crystal sensor successfully received the ultrasound guided waves in a plate-like structure at 800°C. In addition, crack-type damage was approximately localized using the laser-generated ultrasound waves.

Wireless Data Transfer

The wireless data-transfer system was developed and validated with the vibration sensor, as illustrated in Figure 1. The Arduino and the Raspberry Pi were programmed to acquire data accurately at up to 7.5 kHz with just 800 samples. By using the Serial Peripheral Interconnect communication protocol, the Arduino was able to receive the digitized analog data from the Analog to Digital Converter. The Arduino then uses Serial Peripheral Interconnect to communicate the information to the Raspberry Pi. Graphical User Interface was designed using LabVIEW to visualize the Vibration G-force and the frequency of vibration Figure 1. The vibration signal, remotely measured, showed a reliable agreement with the data measured at the oscilloscope, directly connected with the sensor.

Continued on next page

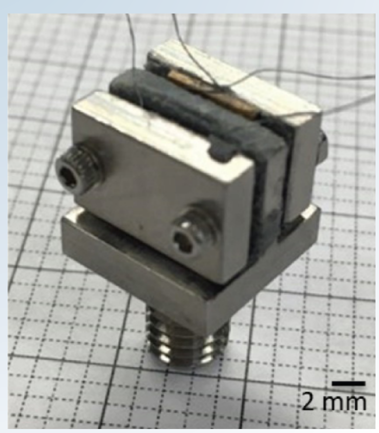

Figure 2. Vibration sensor for NPP application [8].

Continued from previous page

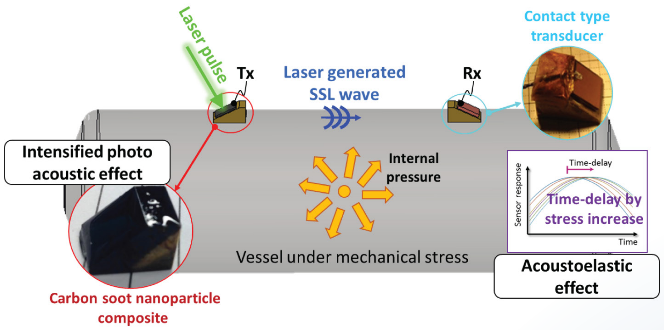

Figure 3. Laser assisted stress sensor [9].

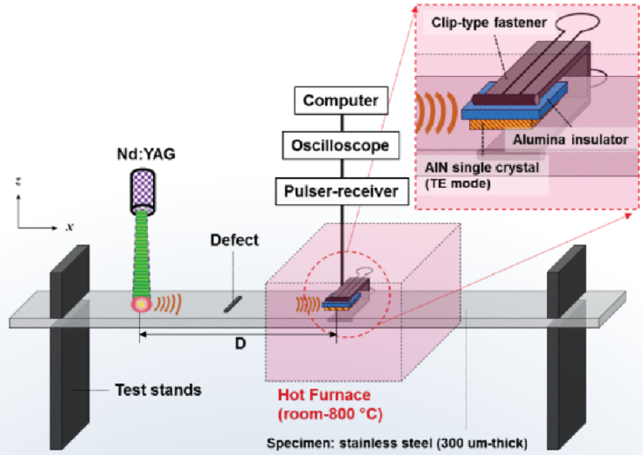

Figure 5. Laser-assisted HT damage detector [10].

Conclusions

The reported HT and radiation-resistant sensors showed that multiple structure parameters can be monitored non-invasively for NPP structures. The reported sensor system detects vibration, mechanical stress, liquid level, and structure damage locations. Moreover, wireless data-transfer technology studied will reduce the effect on humans in an NPP while producing economic benefits during the plant operation. The demonstrated HT and radiation-resistant wireless sensing system is expected to provide safe, economical, reliable sensing options to the modern NPPs.

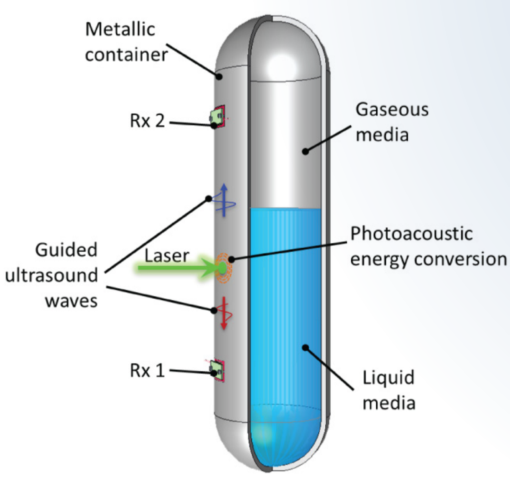

Figure 4. Laser-assisted HT liquid level sensor.

References

[1] Korsah, K., et al. (2009), Instrumentation and Controls in Nuclear Power Plants: An Emerging Technologies Update, Nuclear Regulatory Commission.

[2] Hashemian, H. M., et al. (1989), Effect of Aging on Response Time of Nuclear Plant Pressure Sensors (No. NUREG/CR--5383), Nuclear Regulatory Commission.

[3] Decreton, M., Shikama, T., & Hodgson, E. (2004), Performance of Functional Materials and Components in a Fusion Reactor: The Issue of Radiation Effects in Ceramics and Glass Materials for Diagnostics, J Nuclear Materials, Vol. 329, pp. 125–132.

[4] Lamarsh, J. R., & Baratta, A. J. (2001), Introduction to Nuclear Engineering, Vol. 3, Upper Saddle River, NJ: Prentice hall.

[5] Jiang, X., et al. (2014), High-Temperature Piezoelectric Sensing, Sensors, Vol. 14, No. 1, pp. 144–169.

[6] Wong, K. K. (Ed.). (2002), "Properties of Lithium Niobate," INSPEC, London, UK.

[7] Parks, D. A., and Tittmann, B. R. (2014), "Radiation Tolerance of Piezoelectric Bulk Single-Crystal Aluminum Nitride," IEEE Trans Ultrason Ferroelectr Freq Contro, Vol. 61, No. 7, pp. 1216–1222.

[8] Kim, H., Kerrigan, S., Bourham, M. & Jiang, X. (2020), "AlN Single Crystal Accelerometer for Nuclear Power Plants," IEEE Trans Ind Electron, Submitted for Publication.

[9] Kim, H., Chang, W. Y., Kim, T., & Jiang, X. (2020), "Stress Sensing Method via Laser-Generated Ultrasound Wave Using Candle Soot Nanoparticle Composite," IEEE Tans Ultrason Ferroelectr Freq Control, Submitted for Publication.

[10] Kim, T., Kim, J., & Jiang, X. (2018), "AlN Ultrasound Sensor for Photoacoustic Lamb Wave Detection in a High-Temperature Environment," IEEE Trans Ultrason Ferroelectr Freq Control, Vol. 65, No. 8, pp. 1444–1451.

Development of an Optical Fiber-based Gamma Thermometer

Thomas E. Blue
The Ohio State University

Pavel Tsvetkov
Texas A&M University

Tunc Aldemir
The Ohio State University

Diego Mandelli
Idaho National Laboratory

Introduction

The Optical Fiber-based Gamma Thermometer (OFBGT) project (1) develops an OFBGT that is appropriate for use in University Research Reactors (URRs); (2) tests the OFBGTs in two university research reactors, namely The Ohio State University Research Reactor (OSURR) and the Texas A&M Research Reactor; and (3) develops methods to calculate the volumetric power distribution (and its associated uncertainty) within a URR from the data that is produced by an array of OFBGTs. These goals are intended to be first steps in the development of OFBGTs for application in power reactors.

The rationale for this research project is discussed below with regards to the application of OFBGTs in power reactors, one of which is boiling water reactors (BWR) for which gamma thermometers (GT) that use thermocouples to sense temperatures have been deployed. We will call such GT state-of -the-art GTs (SOA GTs) to distinguish them from the OFBGTs that we are developing. The volumetric power distribution in BWRs is monitored by Local Power Range Monitors (LPRMs). Over time, the LPRMs lose sensitivity due to burnup of the fissionable material, which requires recalibration. Currently, LPRMs are calibrated with traversing in-core probes (TIPs). TIPs are principally similar to LPRMs; they need to be inserted for calibration and removed after calibration to avoid burnup within the TIPs. The process to get a TIP next to each LPRMs is complex and introduces the possibility of a release of radioactive material.

To prevent the release of radioactive materials from the reactor vessel requires a permanent system of sensors in place for LPRM calibration that does not degrade. This would also make the calibration process significantly less difficult and time consuming. SOA GTs are intended to serve this purpose. A SOA GT is composed of an isolated thermal mass, an outer sheath, and a gap between the thermal mass and the sheath. The GT temperature (the temperature of the thermal mass) is monitored by a thermocouple, and a second thermocouple, conceivably, is used to monitor the temperature of the outer sheath. A temperature difference, ΔT, is generated between the thermal mass and outer sheath as a result of the thermal resistance of the gap. Assuming that the relationship between energy deposition rate and ΔT is known, one can acquire a dose rate measurement in the GT. The dose rate measurement in a given GT can be used to calibrate an adjacent LPRM.

A system of GTs for LPRM calibration could be improved by making them optical fiber-based. [1] Utilizing optical frequency domain reflectometry, a distributed temperature measurement can be acquired along an optical fiber. Thus, one can monitor the temperature of a linear array OFBGTs with the same fiber. One could not create a correspondingly dense linear array using SOA GTs, because of cabling concerns.

The OFBGT design is currently under development. In addition, the collaborators on this project are developing a data analytic method that allows the power distribution to be inferred in a reactor core based on the response of an array of OFBGTs in the core. This method makes the developing technology promising for application in many possible reactor types, and not just for LPRM calibration in BWRs. The overall plan is to develop an OFBGT that can be tested in the OSURR and Texas A&M Research Reactor.

Overall Design Description

The OFBGT design is shown in Figure 1. The overall OFBGT design can be broken down into three main parts; the thermal mass, the gas gap, and the outer sheath. The thermal mass is responsible for the gamma heat generation (q_γ). The gas gap provides the dominant thermal resistance, R, out of the three OFBGT regions. A temperature difference, ΔT, is generated across the gas gap between the thermal mass and the outer sheath, as described by:

$$\Delta T = q_\gamma R \qquad (1)$$

Continued on next page

Continued from previous page

The bulk of the thermal mass is a thick quartz glass tube. Within the quartz tube is a mullite insulating tube with four through-holes. Within two of the through holes are two optical fibers: one in each through-hole. A nichrome heating wire travels down the thermal mass and back up the thermal mass, within the other two through-holes. The nichrome wire will be used to calibrate the OFBGT, by supplying a sequence of known energy deposition rates by resistance heating, thus providing the data that is necessary to develop a relationship between ΔT and q_γ. The gas gap is composed of argon and the outer sheath is constructed of aluminum 5052. The temperature of the outer sheath will be monitored by an optical fiber within a stainless-steel capillary tube that is tack welded to the outer sheath. The outer diameter of the OFBGT is 0.5 inches.

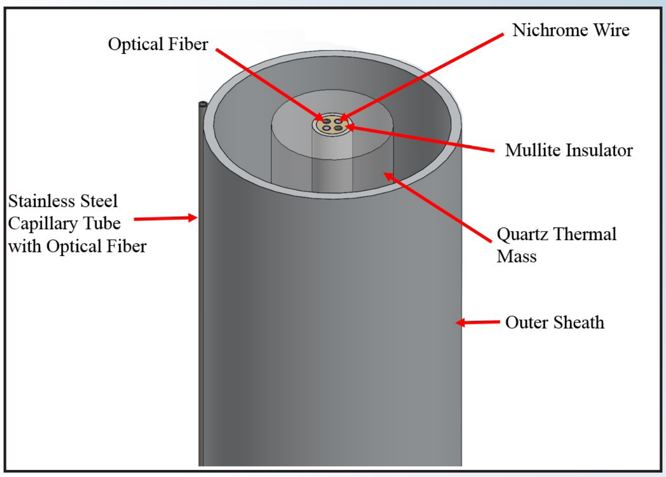

Figure 1. Depiction of the OFBGT design.

Monte Carlo N-Particle Modeling

For the Monte Carlo N-Particle (MCNP) modeling of the OFBGT it is a simplified OFBGT design representation with three regions: a quartz thermal mass, an argon gas gap, and an aluminum outer sheath. In this simplified model, the components are not considered within the thermal mass. The OFBGT is placed within the central irradiation facility (CIF) of the OSURR in the MCNP model. A visual representation of the simple OFBGT within the CIF is shown in Figure 2.

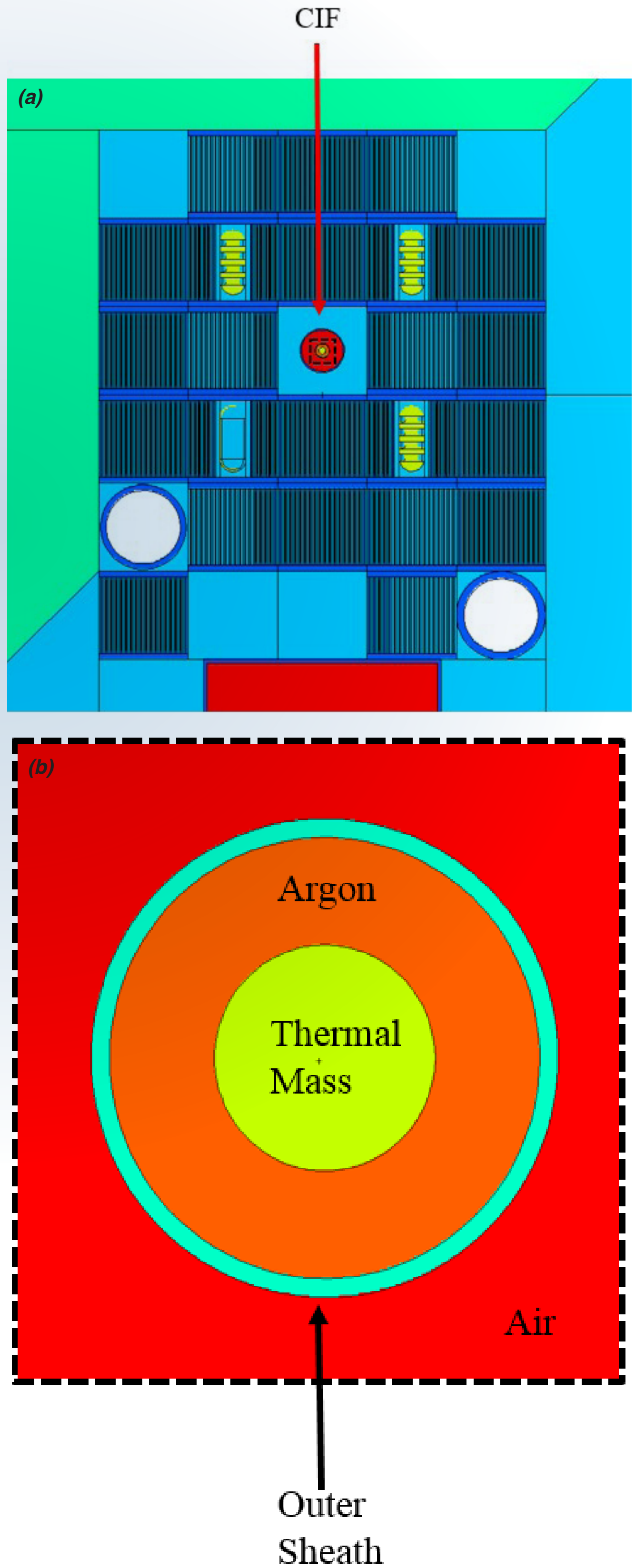

Figure 2. (a) Top-down view showing the simple OFBGT design within the CIF tube in the MCNP model of the OSURR. (b) Close-up view of the simple OFBGT geometry itself.

Continued on next page

Continued from previous page

The energy deposition rate (q''') as a function of axial length was determined for 1-inch-long axial segments for the three regions of the simple OFBGT design. The q''' for the thermal mass and outer sheath is shown in Figure 3. The heat generation in the argon was negligible.

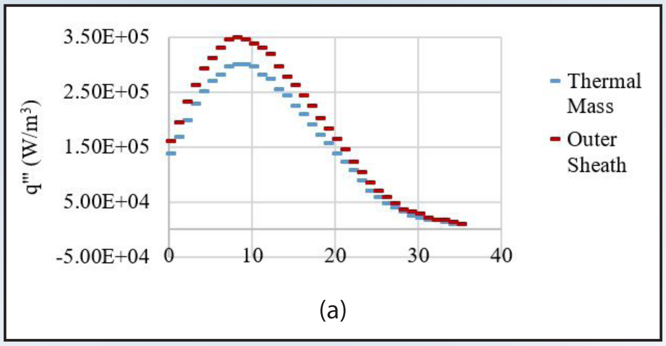

Figure 3. Energy deposition rate in the thermal mass and outer sheath of the OFBGT in the CIF.

Thermal Performance

Knowing the heat generation rate as a function of axial length, we determined the temperature profile in the OFBGT to ensure that the ΔT values are high enough to provide good resolution in the measurement of ΔT, but are not so high that the sensor materials could be damaged. Using an analytical thermal model, [2] the predicted temperature profile of the OFBGT in the CIF of the OSURR has been determined and is shown in Figure 4.

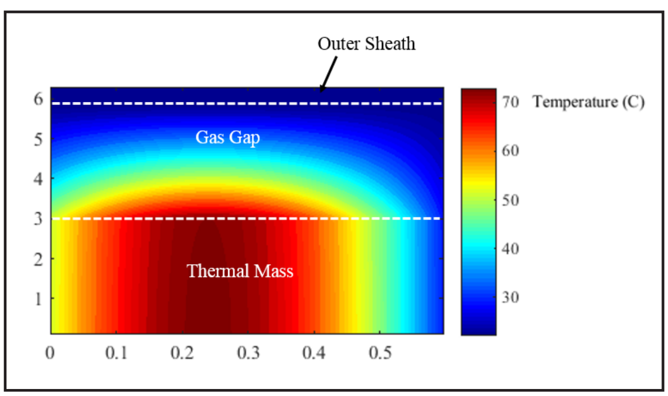

Figure 4. Temperature distribution in the OFBGT in the CIF of the OSURR.

In addition to determining the expected ΔT values in a URR, we also determined the extent to which axial heat conduction modulates the distribution of heat energy. We did so by implementing a modulation transfer function in our analytical model. Our analysis confirms that the modulation is negligible, which means that our calibration error will be low.

Data Analytic Methodology

The data analytic methodology, which is used to process the OFBGT data and to infer the reactor power distribution, is a three-step process. [3] A schematic for this methodology is given in Figure 5. The first step is an energy balance method, which uses modeled data from MCNP and the experimental data from an OFBGT array to acquire power estimates for each OFBGT segment based on response functions. The second step is to average together these estimates, using a weighting scheme, to obtain an updated power profile of the core. The final step is to propagate uncertainty.

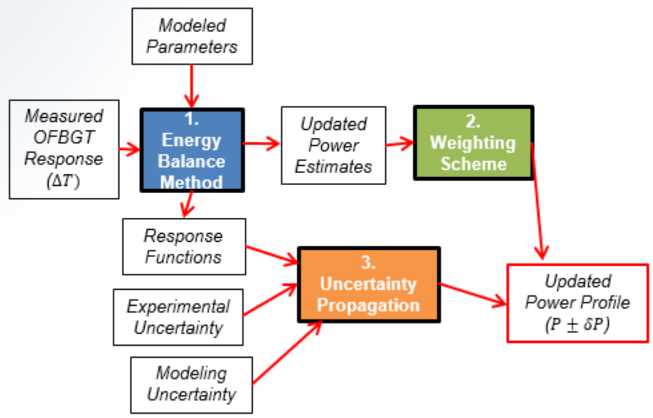

Figure 5. OFBGT data analytic methodology.

Conclusions

The OFBGT design has been described in terms of its energy deposition rate and thermal response. We expect the design to reach an appropriate steady-state temperature and have little calibration error. The data from an array of OFBGTs can be processed to infer the power distribution in a reactor, based on a data analytic methodology that has been developed.

References

[1] Koste, G. P., H. Xia, K. Lee, 2013. Optical Gamma Thermometer. Patent No.: US 8.503,599 B2.

[2] Birri, A., C. M. Petrie, T. E. Blue, "Analytic Thermal Model of an Optical Fiber Based Gamma Thermometer and its Application in a University Research Reactor," IEEE Sensors, to be published, accepted, 2020.

[3] Birri, A., T. E. Blue, "Methodology for Inferring Reactor Core Power Distribution from an Optical Fiber Based Gamma Thermometer Array," Progress in Nuclear Energy, to be published, submitted, 2020.

High Temperature Operable, Harsh Environment Tolerant Flow Sensors for Nuclear Reactor Applications

Jon Lubbers
Sporian Microsystems, Inc.

Laurel Frediani
Sporian Microsystems, Inc.

Motivation and Background

A commonly noted sensor need for Generation-IV nuclear power systems is flow sensing in the coolant or liquid fuel loops in order to monitor fluid velocity and characterize mixing/cooling. The ability to deploy a distribution of flow measurement sensors within the reactor pressure vessel will improve the ability to continuously measure the margin available to reaching design basis limits. This information could be used to allow the reactor to operate at higher temperatures, which would improve the thermal efficiency and allow more electricity to be generated from the same nuclear fuel investment. Such a sensor must be able to tolerate high-temperature, pressure, and radiation (neutron and gamma) environments while being minimally disruptive of the flow.

Flow monitoring is particularly important in small modular reactor (SMR) designs where coolant flow is driven by natural convective flow. In contrast to existing light-water reactors, this is a concern because there are no coolant pumps providing indication and control of flow. A number of other power systems and industrial processes would benefit from high-temperature flow monitoring, including metal production and refining, concentrating solar power systems, and molten salt reactors.

To support SMR development and operations as well as other industries, Sporian Microsystems is developing a flow sensor for use in SMR pressure vessels under a Phase IIB award from the Department of Energy Small Business Innovation Research program.

Technical Approach

Sporian Microsystems specializes in miniaturized, low-power sensor systems for remote environmental monitoring applications, and has previously developed a range of compact sensing technologies for government research and private industry customers. Sporian's sensor technology is based on the combination of advanced ceramics, packaging for harsh environments, and advanced integrated electronics.

Sporian's flow sensor operates on the principle of thermal anemometry. Compared to other types of flowmeters, this approach allows measurement in non-tubular vessels such as the annular downcomer of an SMR. Thermal flow sensors also provide a large range of measurable flow rates that, combined with Sporian's high-temperature-operable probe design, makes the sensor useful in a wide range of harsh systems and processes. While this is not a novel concept, Sporian's patented sensor technology (US #10,436,661) is set apart by its ability to operate at high temperatures (500°C, pushing to 800°C) and pressures (2000 psi and possibly higher) thanks to high-temperature materials and packaging techniques.

More than just a transducer or sensing element, the flow sensing system includes electronics with "smart" signal conditioning approaches, implementing features such as digital communications, internal compensation (temperature), internal calibration (output data in engineering units), and sensor self-identification in a highly integrated (<1 in3) "bump-on-cable" format. Typically, the electronics are physically separated from the probe by a length of rigid (mineral-insulated) or flexible cable as shown in Figure 1, but electronics can also be integrated into the probe head.

Figure 1. Sporian flow sensor with drive electronics.

Continued on next page

Continued from previous page

Results

During Phase II of this effort, Sporian followed an iterative design-build-test cycle to improve reliability and performance, especially with respect to issues of hermeticity, material compatibility, and flow-sensing performance.

- SMR environmental suitability: Prototypes have demonstrated hermeticity and stable output during 100-hour soaks in borated water at 300°C and pressures up to 2300 psi.
- Vibration: Prototypes have passed 20G vibration testing per MIL-STD-810G.
- Thermal shock: Prototypes have passed thermal shock testing between 20°C and 350°C per MIL-STD-810G.
- Thermal cycling: Prototypes have passed thermal cycling testing per MIL-STD-810G with 350 cycles between 20°C and 350°C.
- Accelerated aging: Prototypes have completed functional testing following 650 hours at 550°C, corresponding to approximately 30 years at 300°C. Some drift was observed, but it appears to be predictable.

Flow sensing performance has been characterized in a low-temperature (<100°C) water flow test loop, and performance under different conditions has been estimated based on dimensionless thermal-fluid analysis. Figure 2 shows an example dataset from Sporian's flow sensor compared to a commercial turbine flowmeter. Interestingly, the change from laminar to turbulent flow is detected in the neighborhood of 0.5 m/s. Preliminary performance specifications are summarized in Table 1. The measurement range is limited by the capabilities of the test loop, and it is possible that higher or lower flow velocities will be measurable given improved calibration.

Table 1. Pre-commercial product specifications.

Measurement Range	0.05–1.10 m/s
Accuracy	± 1% FS
Resolution	± 0.01 m/s
Output	0–5 VDC, 4–20 mA, Ethernet
Probe Diameter	0.625 in. (customizable)
Probe Length	5 in. (customizable)

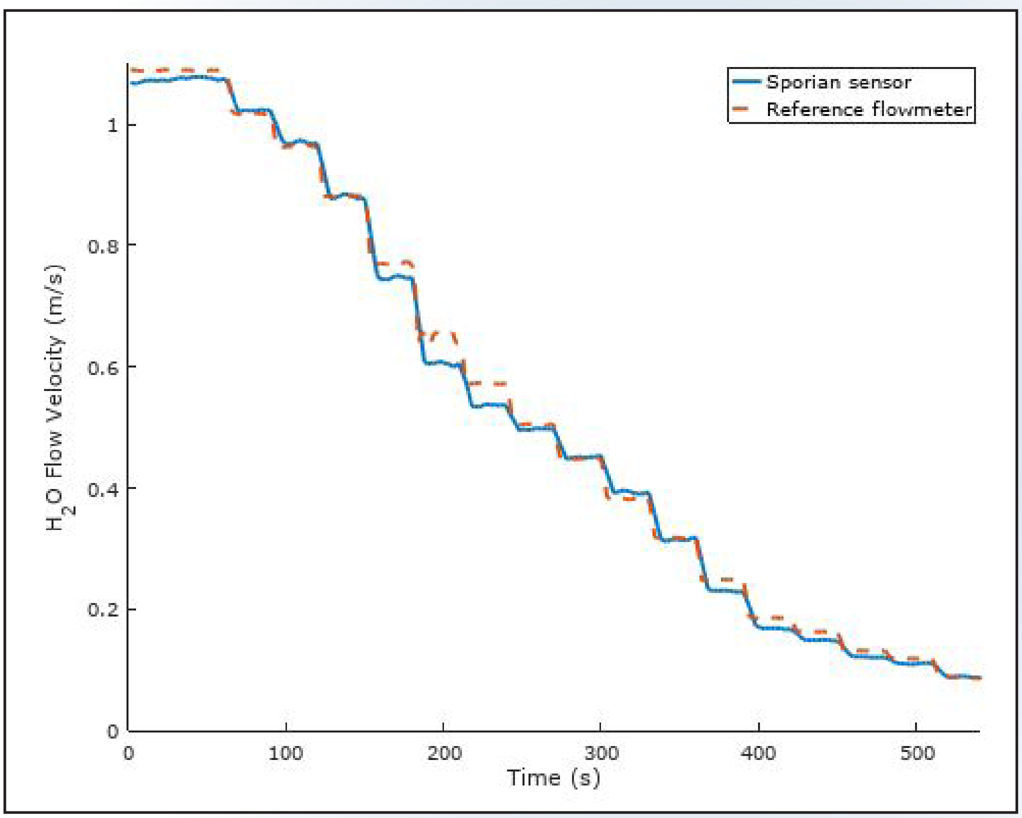

Figure 2. Sporian thermal sensor vs commercial turbine flowmeter, with a transition to turbulence above 0.5 m/s.

Continued on next page

Continued from previous page

Prototype flow sensors have undergone preliminary testing in pressurized water reactor system test loops at Analysis and Measurement Services Corporation, Oregon State University, and Southwest Research Institute.

While prototypes passed these tests, the design and processes are not yet validated across a statistically significant sample size. An important part of Sporian's future work is extensive validation testing in preparation for commercial sales.

Additional Applications

Sporian is adapting this flow sensor technology for use in molten salt systems under a separate Small Business Innovation Research award (Phase II pending). Phase I development consisted of packaging redesign for operation in highly corrosive chloride and fluoride salts at temperatures up to 800°C.

Phase I culminated in a prototype flow sensor being tested in a pumped LiF-BeF2 loop at the University of Wisconsin-Madison. Post-experiment analysis was limited due to beryllium contamination, but there were no signs of damage to the sensor element or packaging.

Status and Availability

This technology is currently in the transition phase from development to commercialization thanks to a Phase IIB award through the Department of Energy. This transition is being accomplished through:

- System risk assessment, including Design Failure Mode and Effects Analysis
- Implementation of quality standards in line with 10 CFR 50, Appendix B, supported by consulting services of United Controls International
- Extensive validation testing at Sporian as well as in third-party system test facilities, including the Critical Heat Flux Test facility at Texas A&M University.

As a small business with finite resources, Sporian's testing capabilities are limited. We are always interested in discussing the possibility of providing sensor systems on an evaluation basis.

This phase of development is scheduled to be completed in the fall of 2021, and commercial sales are expected to begin around the same time.

Acknowledgement

This material is based upon work supported by the U.S. Department of Energy, Small Business Innovation Research (SBIR) and Small Business Technology Transfer (STTR) programs under Award Number DE-SC0013858.

Disclaimer